

Neper/FEPX: free/open-source software packages for finite-element polycrystal plasticity, from microstructure generation to result post-processing

<http://neper.info>, <http://fepx.info>

Romain Quey¹ and Matthew Kasemer²

June 21st, 2021

¹ Laboratoire Georges Friedel, CNRS, MINES Saint-Étienne, France

² University of Alabama, USA



A Brief History

Neper: polycrystal generation and meshing (and more...)

- Developed since 2003, GPL licensed since 2009
- GUI-free, multithreaded (openMP)
- Dependencies: NLOpt, Gmsh, nanoflann, openGJK, libscotch, POV-Ray...

FEPX: parallel finite element polycrystal plasticity

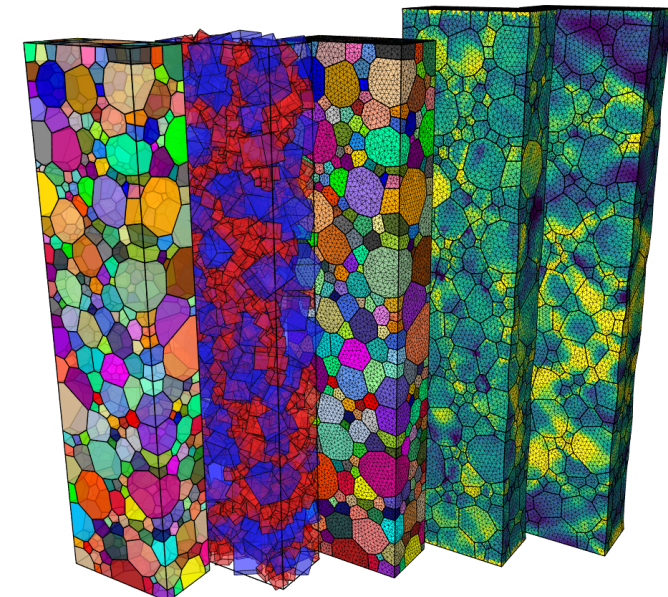
- Developed since the late 90's, GPL licensed since 2020
- Developed in Dawson's group @ Cornell University (USA) until 2019
- GUI-free, parallelized (MPI)

Neper/FEPX

- First common release on July 30th, 2020
- Complete free/open-source solution for finite-element polycrystal plasticity
- Neper's default output is FEPX's default input (and *vice versa*)
- Similar websites, documentations, GitHub repositories, etc.
- Scientific papers (Neper: 3, FEPX: 1 arXiv, Neper/FEPX: in progress)
- Similar “user experiences”

Scientific context (over 20+ years)

(Micro)texture evolution, strain and stress localization, complex microstructures, comparison with X-ray diffraction experiments



Outline

Generation of Microstructures

Meshing

Simulation and Post-processing

Visualization

Conclusions

Outline

Generation of Microstructures

Methodology

Single-scale Microstructures

Multi-scale Microstructures

Other Capabilities

Uniform Crystal Orientation Distributions

Meshing

Simulation and Post-processing

Visualization

Conclusions

Outline

Generation of Microstructures

Methodology

Single-scale Microstructures

Multi-scale Microstructures

Other Capabilities

Uniform Crystal Orientation Distributions

Meshing

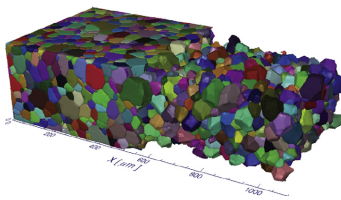
Simulation and Post-processing

Visualization

Conclusions

Microstructure Generation Strategy

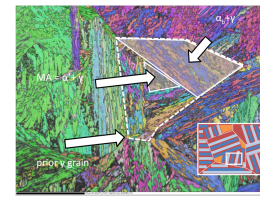
Experimental microstructures



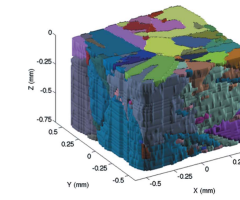
β Ti alloy [Rowenhorst et al., 2010]



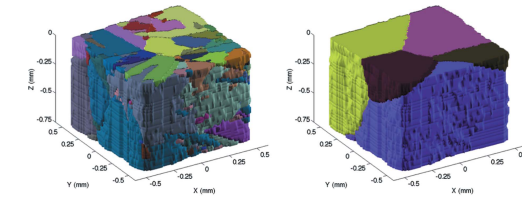
Al alloy [Renversade et al., 2016]



Carbide-free bainitic steel [Hell, 2011]



Lamellar Ti64 & parent β grains [Wieleski et al., 2015]

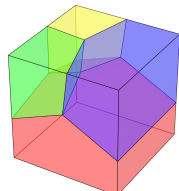


- Grain morphologies (grain size distribution, shapes, ...), orientation distributions
- Grain subdivision, orientation relationships, ... for *multi-scale microstructures*
- Grain-based properties or real morphologies (X-ray diffraction experiments: 3DXRD, DCT, HEDM, ...; TriBeam, ...)

Our numerical microstructures

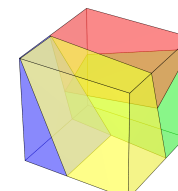
- Convex grains described in a vectorial (CAD-like) format for conventional meshing
- General description, with no extra/superfluous complexity, of 2 types of *microstructures* (topology-wise):

Geometry + optimization



Grains meet along grain boundaries, triple lines and quadruple points
("face-to-face, edge-to-edge and vertex-to-vertex")

Single-scale microstructures → normal tessellations



Grains do not meet along grain boundaries, triple lines and quadruple points
("face-to-face, edge-to-edge and vertex-to-vertex")

Multi-scale microstructures → non-normal tessellations

Outline

Generation of Microstructures

Methodology

Single-scale Microstructures

Multi-scale Microstructures

Other Capabilities

Uniform Crystal Orientation Distributions

Meshing

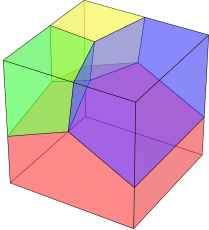
Simulation and Post-processing

Visualization

Conclusions

General Description of Single-scale Tessellations

Normal tessellation (naive description)



- Domain of space, D
- Sets of polyhedra, faces, edges and vertices
- Topological relationships (graph)
- Geometrical relationships (planar faces)



Al alloy [Renversade et al., 2016]

“Every normal tessellation is a Laguerre tessellation (in 3D or more).” [Lautensack, 2007]

Laguerre (weighted-Voronoi) tessellation

- Tessellation of D into cells, C_i , from seeds, $S_i(x_i, w_i)$, such that

$$C_i = \left\{ P(x) \in D \mid d(x, x_i)^2 - w_i < d(x, x_j)^2 - w_j \quad \forall j \neq i \right\}$$

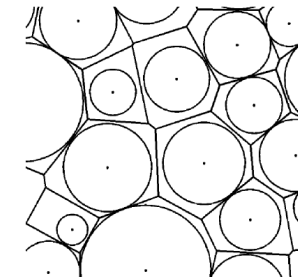
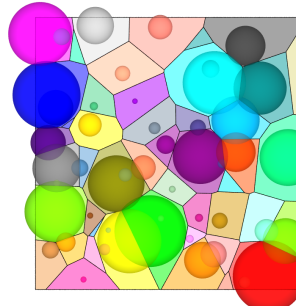
N cells $\rightarrow 4N$ variables

The larger the weight, the bigger the cell

Seeds may not belong to their cells, cells may be void

- Almost always coupled to dense sphere packing,
but this breaks their generality

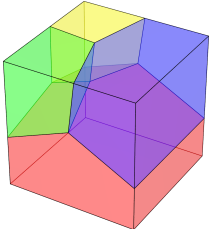
General Laguerre tessellations demand independent x_i and w_i



[Fan et al, 2004]

General Description of Single-scale Tessellations

Normal tessellation (naive description)



- Domain of space, D
- Sets of polyhedra, faces, edges and vertices
- Topological relationships (graph)
- Geometrical relationships (planar faces)



Al alloy [Renversade et al., 2016]

“Every normal tessellation is a Laguerre tessellation (in 3D or more).” [Lautensack, 2007]

Laguerre (weighted-Voronoi) tessellation

- Tessellation of D into cells, C_i , from seeds, $S_i(x_i, w_i)$, such that

$$C_i = \left\{ P(x) \in D \mid d(x, x_i)^2 - w_i < d(x, x_j)^2 - w_j \quad \forall j \neq i \right\}$$

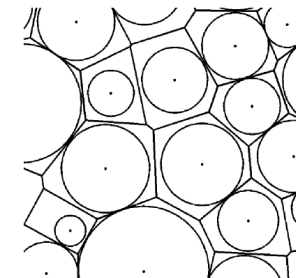
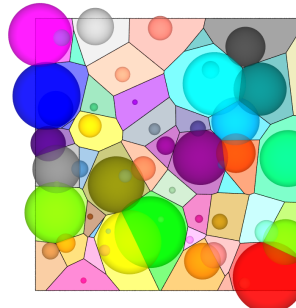
N cells $\rightarrow 4N$ variables

The larger the weight, the bigger the cell

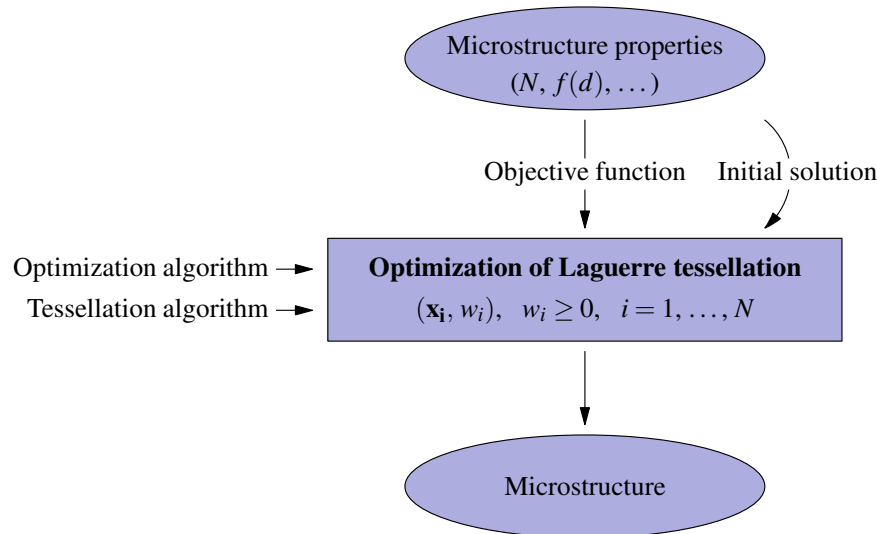
Seeds may not belong to their cells, cells may be void

- Almost always coupled to dense sphere packing,
but this breaks their generality

General Laguerre tessellations demand independent x_i and w_i



[Fan et al, 2004]

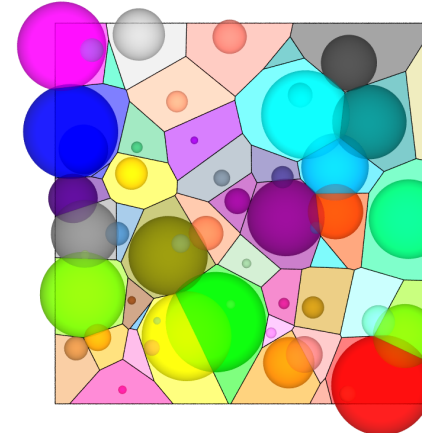


Optimization algorithm

- Non-linear, local, gradient-free and large-scale → Subplex and Praxis from NLOpt
- Number of iterations $O(N)$
- 1-3 variables changed from one iteration to the next

Tessellation algorithm / Option 1: full tessellation computation

- Computation of all cells: time in $O(N \log N)$
 - Computation of the objective function: time in $O(N)$
- Total time in $O(N^2 \log N)$ 



Optimization algorithm

- Non-linear, local, gradient-free and large-scale → Subplex and Praxis from NLOpt
- Number of iterations $O(N)$
- 1-3 variables changed from one iteration to the next

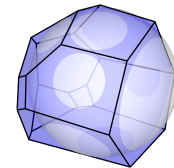
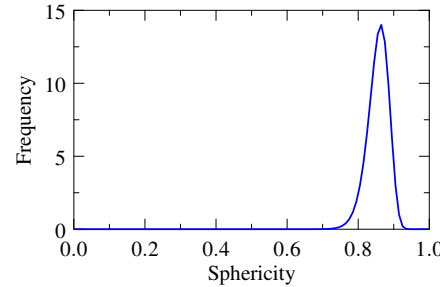
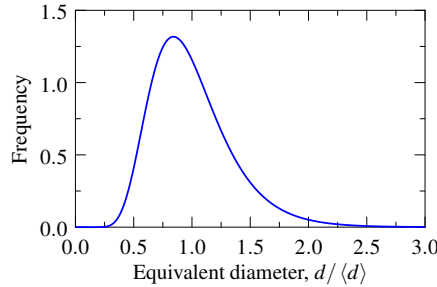
Tessellation algorithm / Option 1: full tessellation computation

- Computation of all cells: time in $O(N \log N)$
 - Computation of the objective function: time in $O(N)$
- Total time in $O(N^2 \log N)$ 

Tessellation algorithm / Option 2: local tessellation update

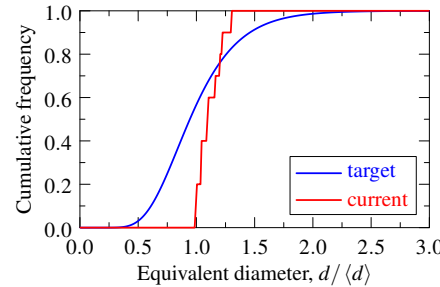
- Computation of 10–20 cells: time in $O(\log N)$
 - Update of the objective function: time in $O(1)$
- Total time in $O(N \log N)$ 

Microstructure Properties



Objective function

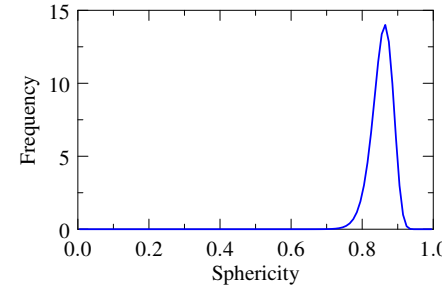
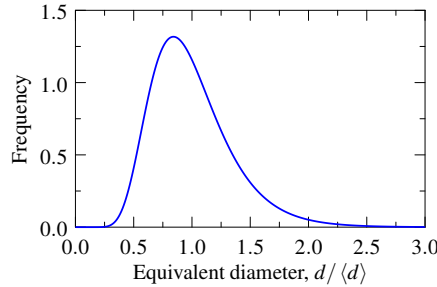
- Adaptation of the Anderson-Darling test (1952)
- For each variable: $\mathcal{O} = \int_{-\infty}^{+\infty} \frac{(F^*(x) - F(x))^2}{F(x)(1-F(x))} dx$
- In total: $\mathcal{O} = \sqrt{\mathcal{O}_{size}^2 + \mathcal{O}_{sphericity}^2}$



Initial solution: Voronoi tessellation

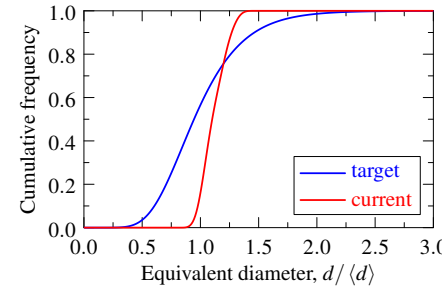
- x_i : random
- w_i : constant = $\langle r \rangle^2$

Microstructure Properties



Objective function

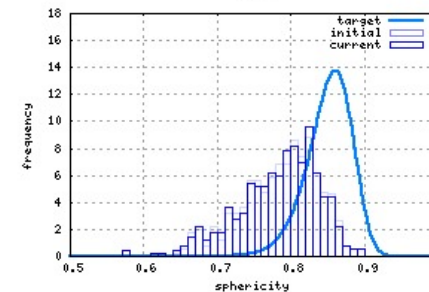
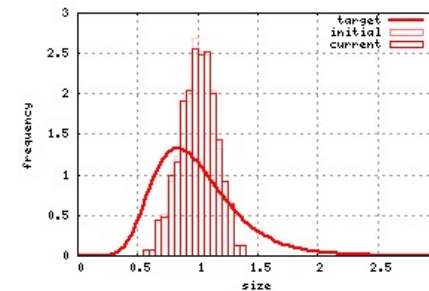
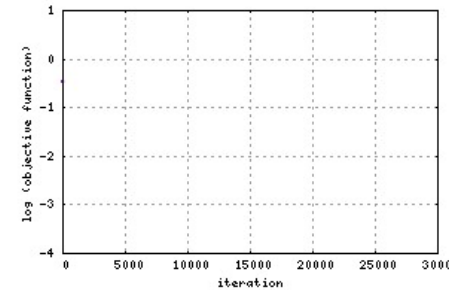
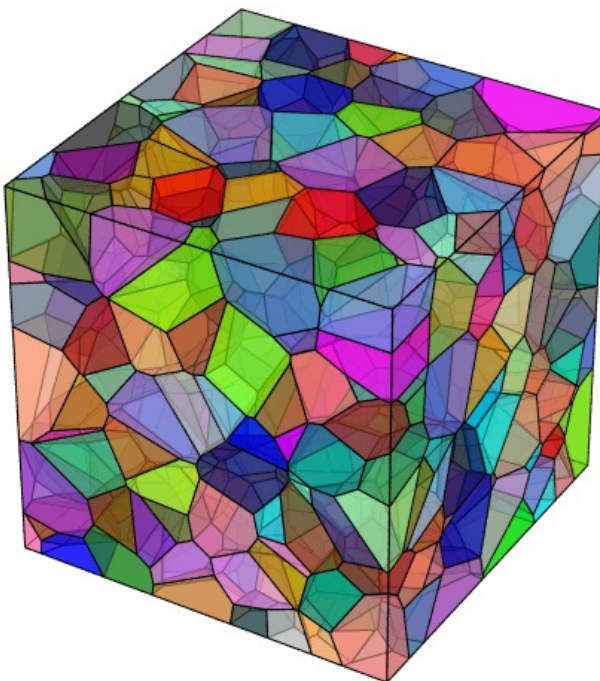
- Adaptation of the Anderson-Darling test (1952)
- For each variable: $\mathcal{O} = \int_{-\infty}^{+\infty} \frac{(F_s^*(x) - F_s(x))^2}{F_s(x) (1 - F_s(x))} dx$
 $F_s^{(*)}(x) = F^{(*)} \circ S$, S : normal distribution
- In total: $\mathcal{O} = \sqrt{\mathcal{O}_{size}^2 + \mathcal{O}_{sphericity}^2}$



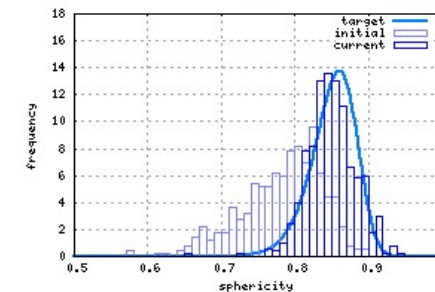
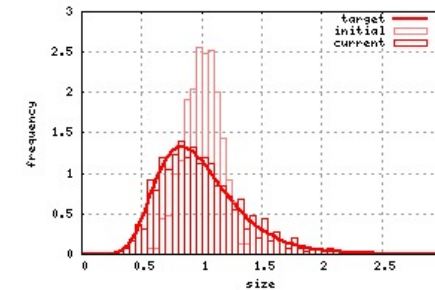
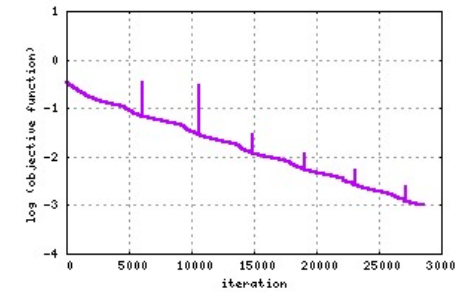
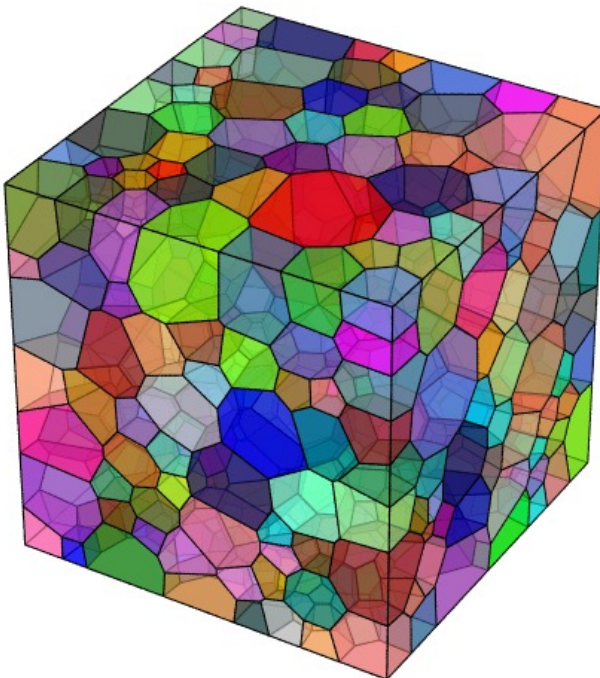
Initial solution: Voronoi tessellation

- x_i : random
- w_i : constant = $\langle r \rangle^2$

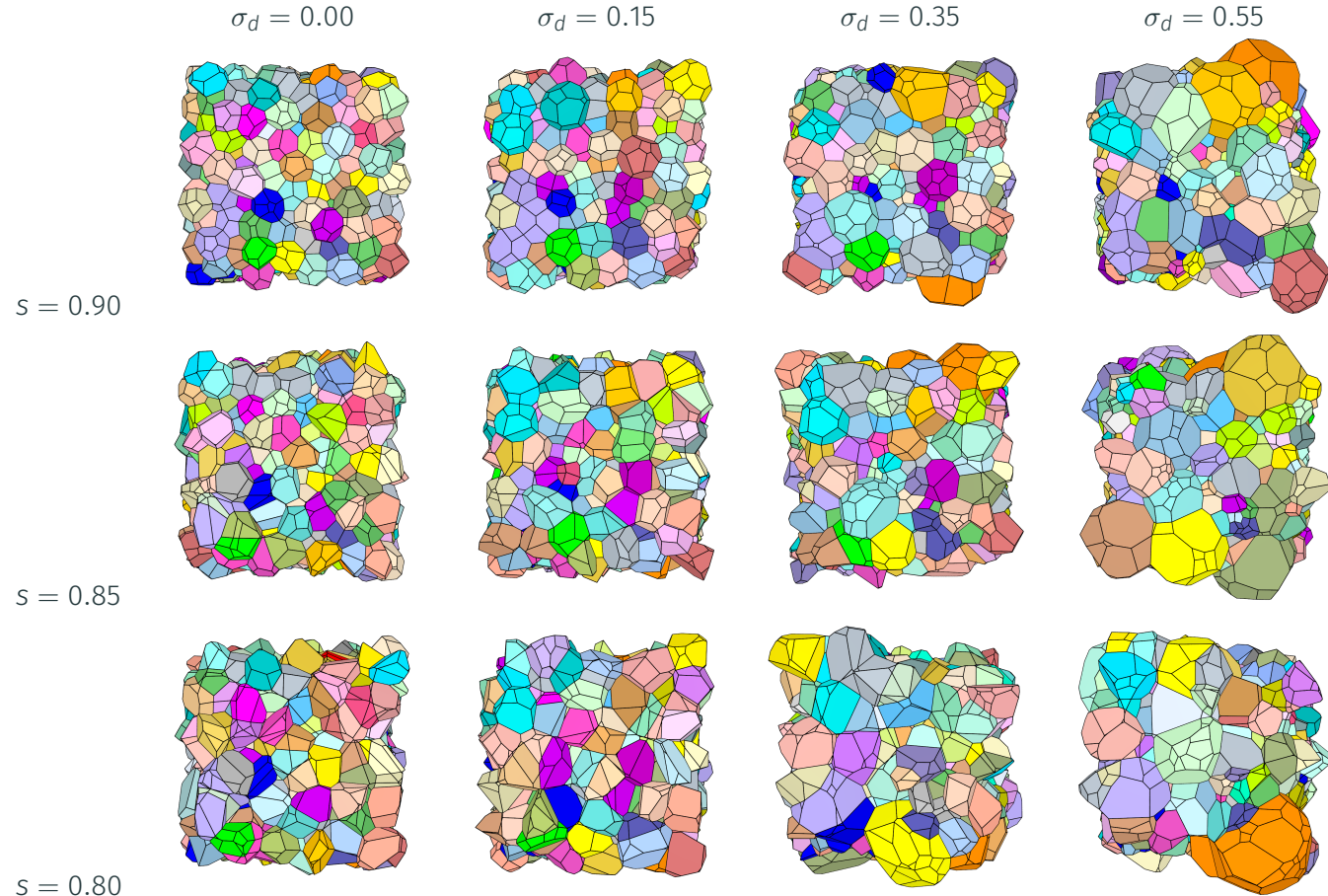
Optimization



Optimization

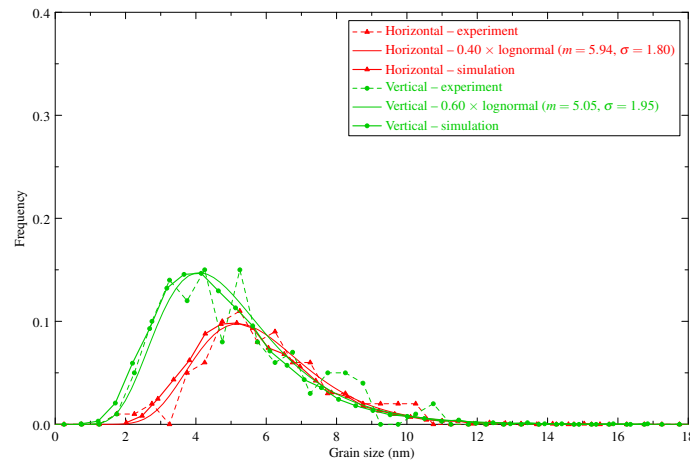


Polycrystals of Varying Properties

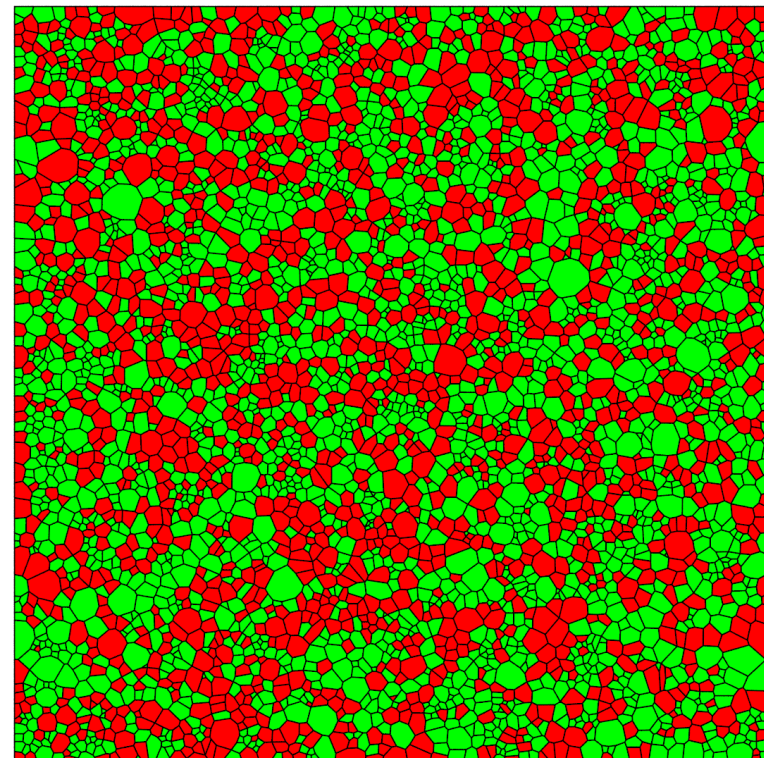


Two-phase Microstructures

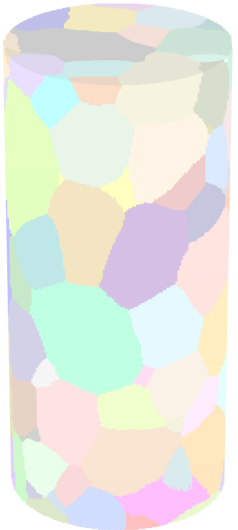
Grain size distributions



Microstructure

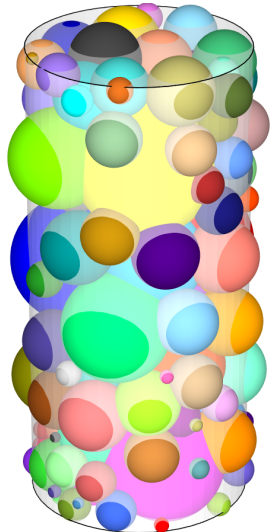


Microstructure properties

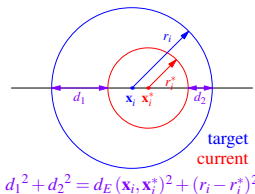


DCT data → ff-3DXRD data

Grain centroids and volumes → spheres
(courtesy H. Proudhon)



Objective function



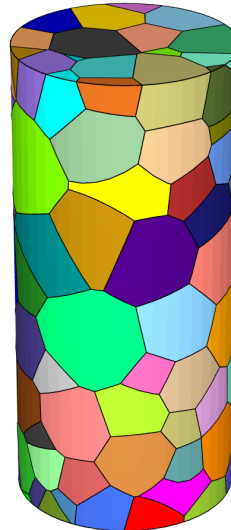
$$\mathcal{O} = \frac{1}{N \langle d \rangle} \sum_i (d_1^2 + d_2^2)$$

Initial solution

\mathbf{x}_i = grain centroid

$w_i = (\text{grain radius})^2$

Microstructure



Initial solution:

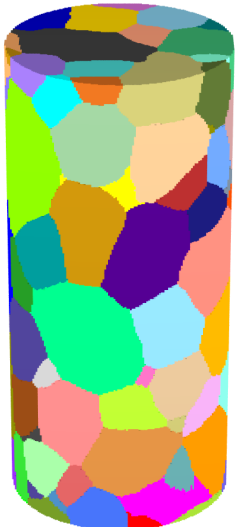
$$\mathcal{O} = 0.0149$$



Final solution:

$$\mathcal{O} = 0.00263$$

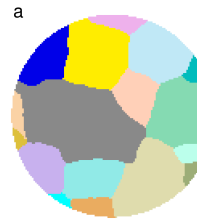
Microstructure properties



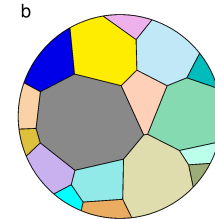
DCT polycrystal

(courtesy H. Proudhon)

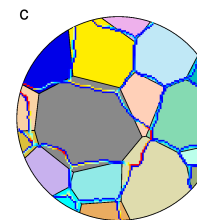
Objective function



polycrystal

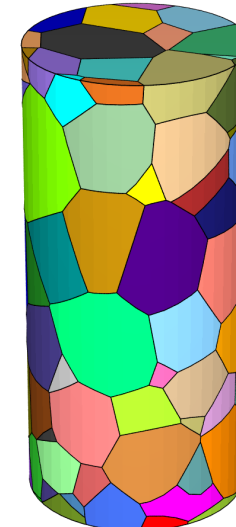


tessellation



distance (boundary points)

Microstructure

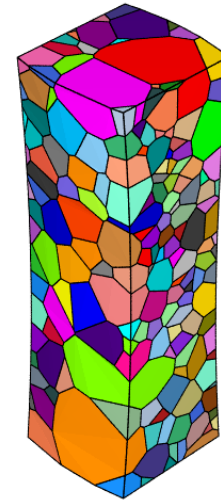
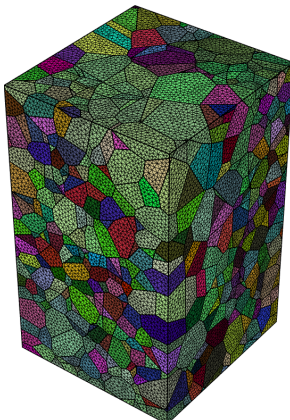
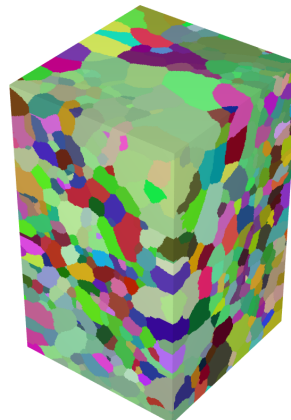
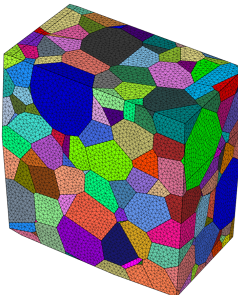
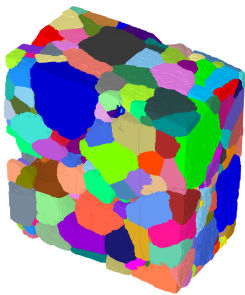


Final solution:

5.6% difference

$$\mathcal{O} = \frac{2}{n_v \langle d \rangle} \sum_{i=1}^N \sum_{v_k \in G_i^b} d_E(v_k, C_i)^2$$

Other examples



DCT data courtesy É. Héripé and A. Dimanov, France

(Quey and Renversade, 2019)

3DPLASTICITY ANR project

- 👍 Adapted to noisy data
- 👍 Robust even for large polycrystals
- 👍 Fully-automated

Outline

Generation of Microstructures

Methodology

Single-scale Microstructures

Multi-scale Microstructures

Other Capabilities

Uniform Crystal Orientation Distributions

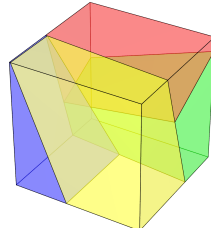
Meshing

Simulation and Post-processing

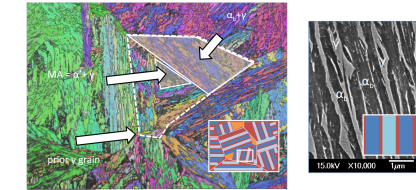
Visualization

Conclusions

Multiscale microstructures (pearlitic / bainitic steels, lamellar Ti64, multilayer materials, ...)



- Characterized by grain subdivisions
- Grains *do not* meet along grain boundaries, triple lines and quadruple points (“face-to-face, edge-to-edge and vertex-to-vertex”)



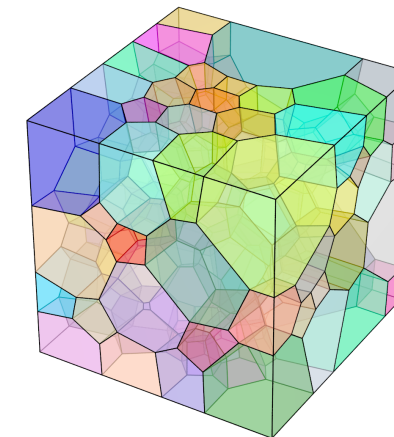
Carbide-free bainitic steel [Hell, 2011]

Non-normal tessellations \Rightarrow cannot be represented by a Laguerre tessellation

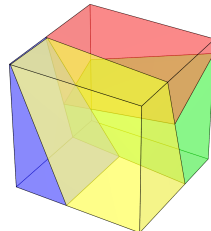
Principle: replicating material’s history

Example of bainitic steel:

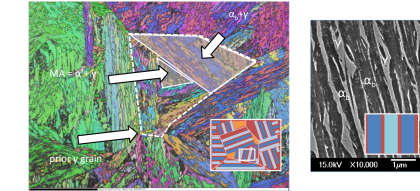
- Scale 1: grain-growth statistics, random orientations
- Scale 2, in each cell:
 - Morphology: seeds on GBs + Voronoi tessellation
 - Orientations: Kurdjumov-Sachs (KS), Nishiyama-Wasserman (NW), ...
- Scale 3, in each cell: lamellae



Multiscale microstructures (pearlitic / bainitic steels, lamellar Ti64, multilayer materials, ...)



- Characterized by grain subdivisions
- Grains *do not* meet along grain boundaries, triple lines and quadruple points (“face-to-face, edge-to-edge and vertex-to-vertex”)



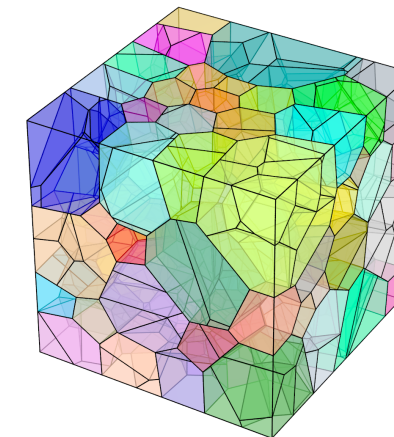
Carbide-free bainitic steel [Hell, 2011]

Non-normal tessellations \Rightarrow cannot be represented by a Laguerre tessellation

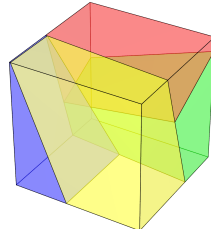
Principle: replicating material’s history

Example of bainitic steel:

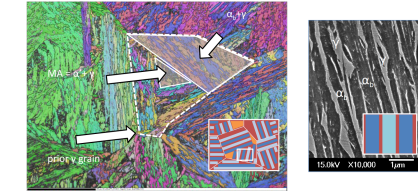
- Scale 1: grain-growth statistics, random orientations
- Scale 2, in each cell:
 - Morphology: seeds on GBs + Voronoi tessellation
 - Orientations: Kurdjumov-Sachs (KS), Nishiyama-Wasserman (NW), ...
- Scale 3, in each cell: lamellae



Multiscale microstructures (pearlitic / bainitic steels, lamellar Ti64, multilayer materials, ...)



- Characterized by grain subdivisions
- Grains *do not* meet along grain boundaries, triple lines and quadruple points (“face-to-face, edge-to-edge and vertex-to-vertex”)



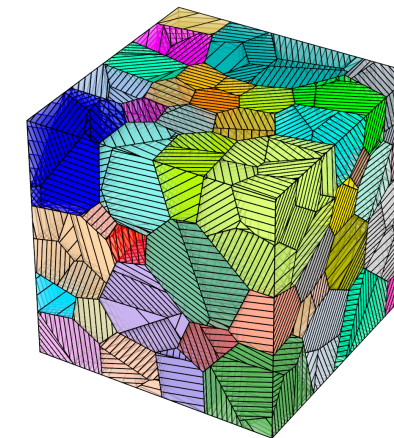
Carbide-free bainitic steel [Hell, 2011]

Non-normal tessellations \Rightarrow cannot be represented by a Laguerre tessellation

Principle: replicating material's history

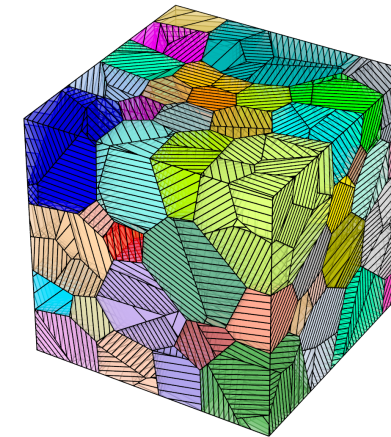
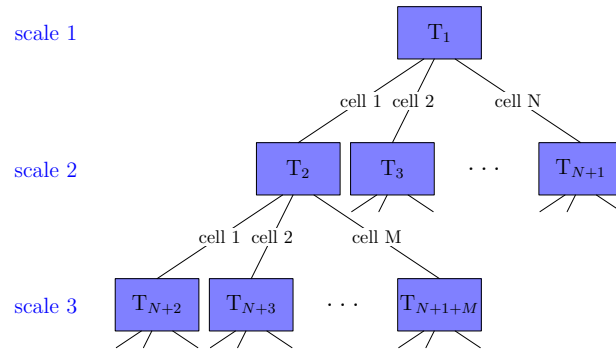
Example of bainitic steel:

- Scale 1: grain-growth statistics, random orientations
- Scale 2, in each cell:
 - Morphology: seeds on GBs + Voronoi tessellation
 - Orientations: Kurdjumov-Sachs (KS), Nishiyama-Wasserman (NW), ...
- Scale 3, in each cell: lamellae

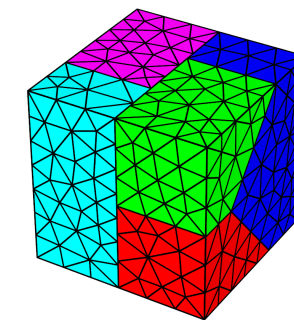
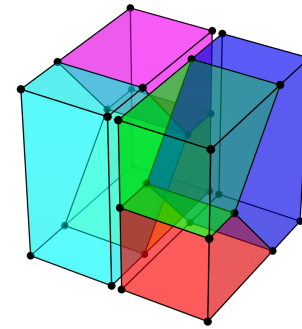
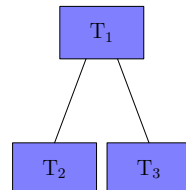


Multiscale Tessellations

Description

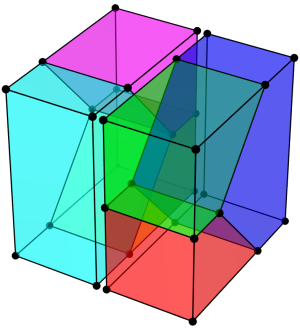


Meshing

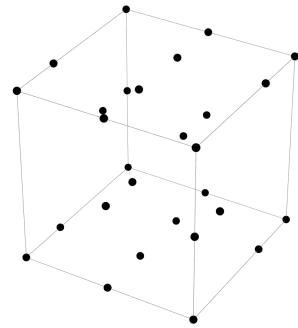


Tessellation Flattening

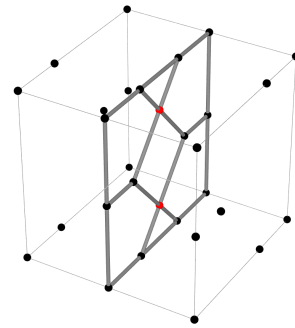
2-scale tessellation



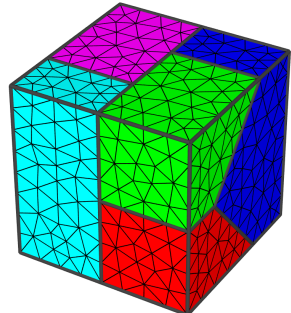
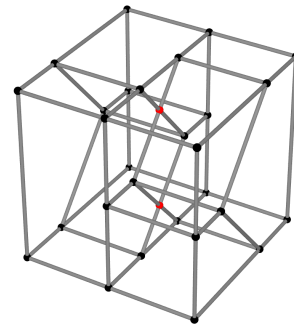
0. multiscale tessellation



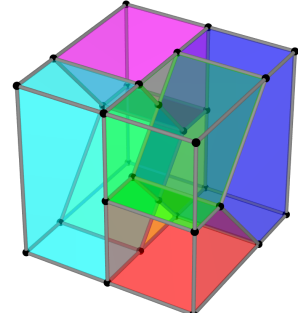
1. vertices: merging



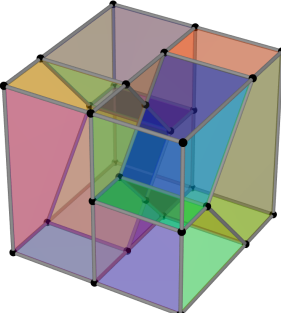
2. edges: intersection + decomposition



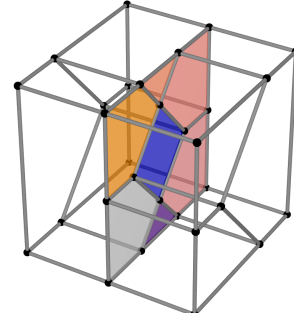
5. final mesh



4. polyhedra

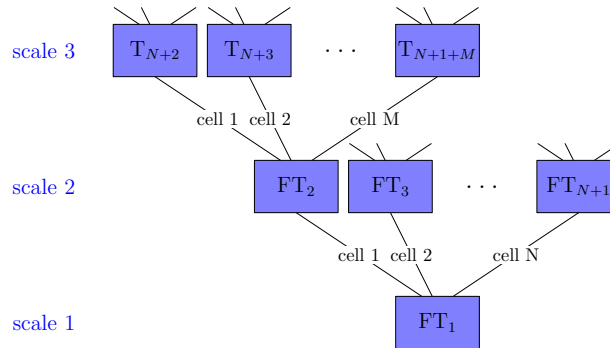


3. faces: decomposition

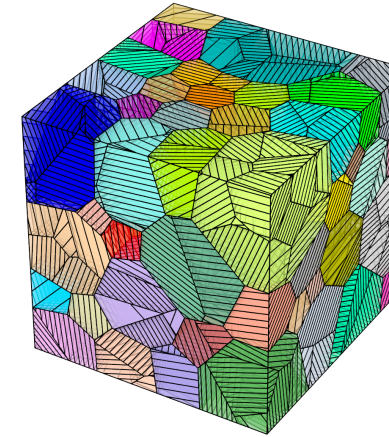


Tessellation Flattening

N-scale tessellation

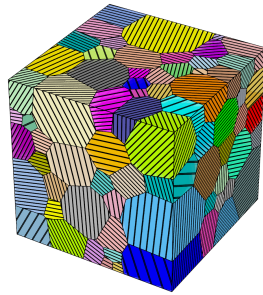


Sequential flattenings down to a unique tessellation

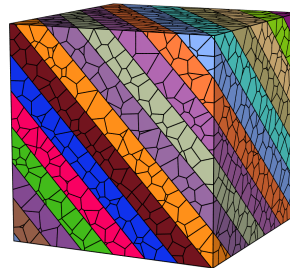


Examples of Multiscale Microstructures

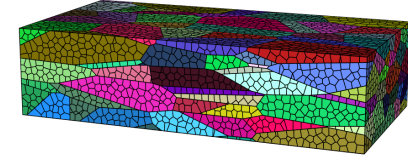
2-scale microstructures



Pearlitic steel

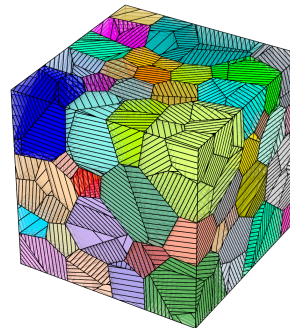


Rocks



Rolled polycrystal (grains / subgrains)

3-scale microstructures



Bainitic steel

Outline

Generation of Microstructures

Methodology

Single-scale Microstructures

Multi-scale Microstructures

Other Capabilities

Uniform Crystal Orientation Distributions

Meshing

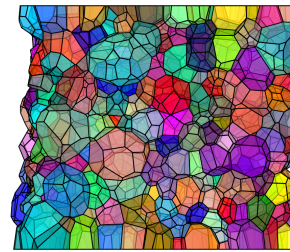
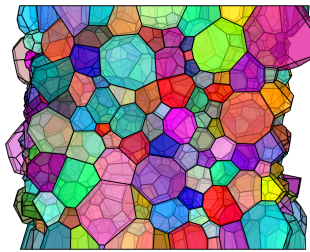
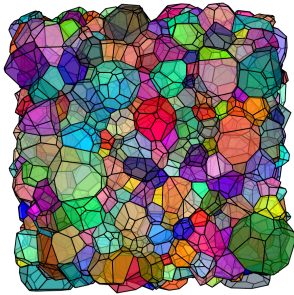
Simulation and Post-processing

Visualization

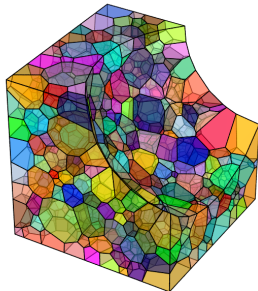
Conclusions

Other Capabilities

Periodicity



Non-convex domains



and much more... (using custom objective functions or seed distributions)

Outline

Generation of Microstructures

Methodology

Single-scale Microstructures

Multi-scale Microstructures

Other Capabilities

Uniform Crystal Orientation Distributions

Meshing

Simulation and Post-processing

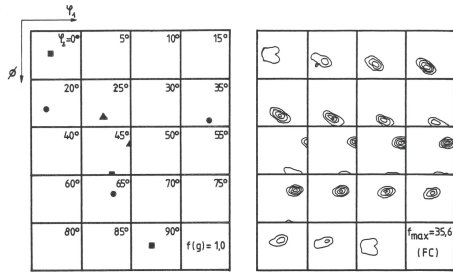
Visualization

Conclusions

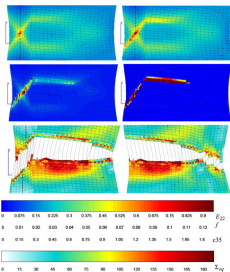
Context

Texture and forming simulations

(Ruer, 1970), (Vadon, 1976), (Montheillet, 1985), (Fortunier, 1987), (Cailletaud, 1988),
(Pilvin and Bacroix, 1991), (Rousselier, 2004), (Raabe and Roters, 2004)

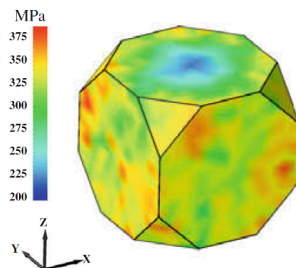


(Fortunier, 1987)

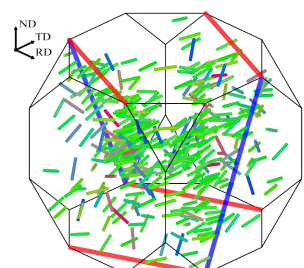


(Rousselier and Luo, 2014)

Analysis of orientation dependency



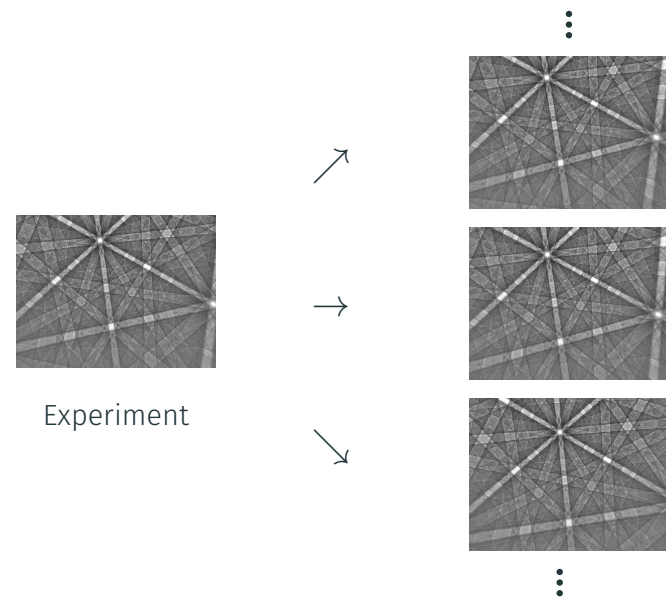
Axial stress (Wong and Dawson, 2009)



Orientation spreads (Quey et al, 2015)

Dictionary-based indexing of diffraction patterns

(Rauch and Véron, 2014), (Suter et al, 2006)
(Singh and De Graef, 2016)

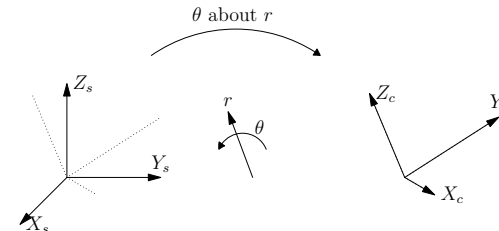


Experiment

Dictionary
(10^5 – 10^6 orientations)

Euler's theorem (Euler, 1775) (in contemporary terms)

"Any orientation can be described by a rotation of angle $\theta \in [0, \pi]$ around a unique axis r ($\|r\| = 1$)."



Quaternions (Hamilton, 1844)

$$q = \cos\left(\frac{\theta}{2}\right) + r \sin\left(\frac{\theta}{2}\right)$$

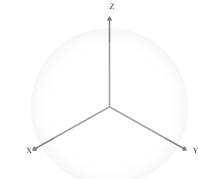
- 4D vectors, $\|q\| = 1, q \in \mathbb{S}^3$
- $(r, \theta) \rightarrow q \equiv (r, \theta + 2\pi) \rightarrow -q$
 $\Rightarrow 1$ orientation = 2 opposite quaternions
- $q_3 = q_1 q_2, q_m = q_2 q_1^{-1}, q^k = q u^k \dots$
- Misorientation angle = 2× intrinsic distance between quaternions
 \Rightarrow no distortion

Uniform orientation distribution \equiv uniform distribution of points on \mathbb{S}_+^3

Graphical representation

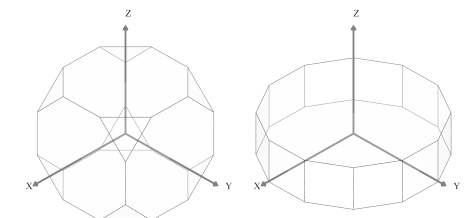
Homochoric projection if no crystal symmetry

$$x_h = r \left(\frac{3}{4} (\theta - \sin \theta) \right)^{\frac{1}{3}}$$



Rodrigues vector if crystal symmetry

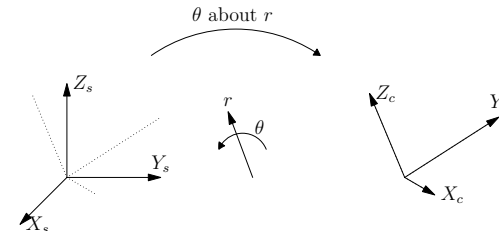
$$x_R = r \tan\left(\frac{\theta}{2}\right)$$



3D Orientation Description using Unit Quaternions and more...

Euler's theorem (Euler, 1775) (in contemporary terms)

"Any orientation can be described by a rotation of angle $\theta \in [0, \pi]$ around a unique axis r ($\|r\| = 1$)."



Quaternions (Hamilton, 1844)

$$q = \cos\left(\frac{\theta}{2}\right) + r \sin\left(\frac{\theta}{2}\right)$$

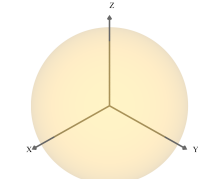
- 4D vectors, $\|q\| = 1, q \in \mathbb{S}^3$
- $(r, \theta) \rightarrow q \equiv (r, \theta + 2\pi) \rightarrow -q$
 $\Rightarrow 1$ orientation = 2 opposite quaternions
- $q_3 = q_1 q_2, q_m = q_2 q_1^{-1}, q^k = q u^k \dots$
- Misorientation angle = 2× intrinsic distance between quaternions
 \Rightarrow no distortion

Uniform orientation distribution \equiv uniform distribution of points on \mathbb{S}_+^3

Graphical representation

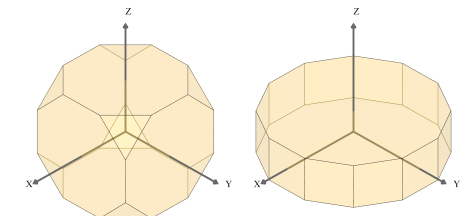
Homochoric projection if no crystal symmetry

$$x_h = r \left(\frac{3}{4} (\theta - \sin \theta) \right)^{\frac{1}{3}}$$



Rodrigues vector if crystal symmetry

$$x_R = r \tan\left(\frac{\theta}{2}\right)$$



Formulation (in contemporary terms)

“Determine the minimum electrostatic potential energy configuration of N electrons constrained to the surface of a unit sphere that repel each other with a force given by Coulomb’s law”

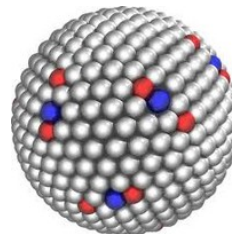


J.J. Thomson
(1856–1940)

1906 Nobel prize

A well-known mathematical problem

- S. Smale's 7th unsolved problem
 - Various resolution methods: gradient-descent optimization, global optimization, ..., genetic algorithms
 - Solutions known for $N = 1, 2, 3, 4, 5, 6$ and 12
 - Focus on $N \leq 1000$, minimal energy, and arrangement faults (dislocations)
 - Number of local minima in $O(e^N)$ (!), but all close to the global minimum



<http://www.quora.com/topic/Thomson-Problem>

STEVE SMALE

Mathematical Problems for the Next Century¹

V. I. Arnol'd, on behalf of the International Mathematical Union, has written to a number of mathematicians with a suggestion that they deserve some great preference for the next century. This report is his response.

Arnol'd's invitation is implicit for all mathematicians of the time to work on problems that have been chosen by him. He has chosen problems, with whom chance does this time.

1. Simple statements. And, probably, mathematically profound.

2. Proved inequalities, also problems. I have not thought about them.

3. I belief that the questions, in statistics, partial orders, combinatorics, etc., are very important. I believe that there is a preference for mathematics and its development in the direction of probability theory.

Some of these problems are simple, (in fact, defined by one sentence), others are complex. The first problem of mathematics is the Riemann Hypothesis, the Fermat Conjecture, the Poincaré Conjecture, the Hodge Conjecture, the Yang-Mills Conjecture, the Poincaré Hypothesis, our below in it follows the Hilbert's 10th Problem, the Ramanujan Conjecture, the Goldbach Conjecture, etc. These are problems, perhaps a little more difficult than the first three.

1. Some of these problems are simple, (in fact, defined by one sentence), others are complex. The first problem of mathematics is the Riemann Hypothesis, the Fermat Conjecture, the Poincaré Conjecture, the Hodge Conjecture, the Yang-Mills Conjecture, the Poincaré Hypothesis, our below in it follows the Hilbert's 10th Problem, the Ramanujan Conjecture, the Goldbach Conjecture, etc. These are problems, perhaps a little more difficult than the first three.

2. Some of these problems are simple, (in fact, defined by one sentence), others are complex. The first problem of mathematics is the Riemann Hypothesis, the Fermat Conjecture, the Poincaré Conjecture, the Hodge Conjecture, the Yang-Mills Conjecture, the Poincaré Hypothesis, our below in it follows the Hilbert's 10th Problem, the Ramanujan Conjecture, the Goldbach Conjecture, etc. These are problems, perhaps a little more difficult than the first three.

3. Some of these problems are simple, (in fact, defined by one sentence), others are complex. The first problem of mathematics is the Riemann Hypothesis, the Fermat Conjecture, the Poincaré Conjecture, the Hodge Conjecture, the Yang-Mills Conjecture, the Poincaré Hypothesis, our below in it follows the Hilbert's 10th Problem, the Ramanujan Conjecture, the Goldbach Conjecture, etc. These are problems, perhaps a little more difficult than the first three.

Problem 1: The Riemann Hypothesis

The Riemann Hypothesis is the conjecture that the non-trivial zeros of the Riemann zeta function, defined by an analytic continuation

$$\zeta(s) = \sum_{n=1}^{\infty} \frac{1}{n^s}, \quad \text{for } s = \sigma + it, \quad \text{where } \sigma > 1,$$

are all located on the line $\sigma = 1/2$ in the complex s -plane. There are many fine books on the non-trivialities and the Riemann Hypothesis.

Problem 2: The Positive Octahedron

Let \mathcal{O} be the positive octahedron in \mathbb{R}^3 . Let \mathcal{O}' be the same octahedron, but with the origin removed. Let \mathcal{O} and \mathcal{O}' meet at the point $(1, 1, 1)$ in their ℓ_1 line. Then there are many fine books on the non-trivialities and the Riemann Hypothesis.

Problem 3: The Positive Octahedron

Let \mathcal{O} be the positive octahedron in \mathbb{R}^3 . Let \mathcal{O}' be the same octahedron, but with the origin removed. Let \mathcal{O} and \mathcal{O}' meet at the point $(1, 1, 1)$ in their ℓ_1 line. Then there are many fine books on the non-trivialities and the Riemann Hypothesis.

$$\mathcal{O} = \{x \in \mathbb{C}^3 \mid |x| = 1\} = \left\{ x \in \mathbb{R}^3 \mid \sum_{i=1}^3 |x_i| = 1 \right\}.$$

A complete and detailed mathematical proof of the Riemann Hypothesis would be a welcome addition to the literature.

¹Some of these problems are simple, (in fact, defined by one sentence), others are complex. The first problem of mathematics is the Riemann Hypothesis, the Fermat Conjecture, the Poincaré Conjecture, the Hodge Conjecture, the Yang-Mills Conjecture, the Poincaré Hypothesis, our below in it follows the Hilbert's 10th Problem, the Ramanujan Conjecture, the Goldbach Conjecture, etc. These are problems, perhaps a little more difficult than the first three.

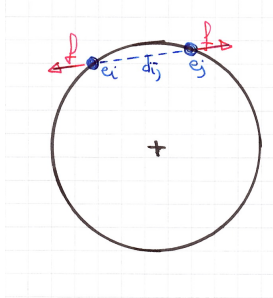
Downloaded from arxiv.org by the Institute of Mathematics, the Hebrew University, Jerusalem, Israel on June 20, 2019.

arXiv:1803.03269v1 [math.HO] 12 Mar 2018

The Thomson Problem for Unit Quaternions: Principle for 2 Orientations

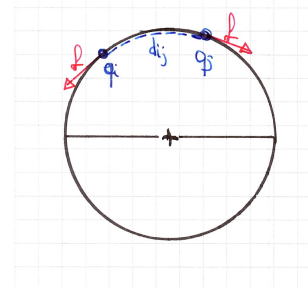
Interaction

Electrons



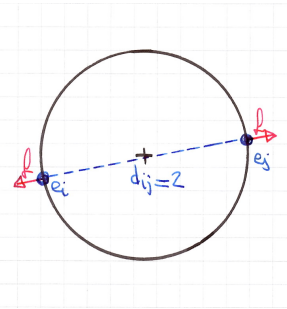
Forces along straight lines in \mathbb{R}^3 ,
1 electron = 1 point

Unit quaternions

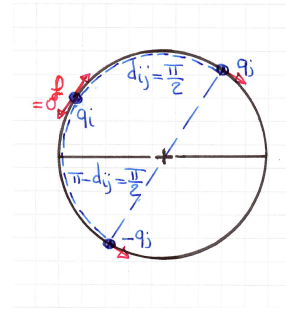


Distances / forces along geodesics of \mathbb{S}^3 1 orientation = 2 antipodal points
Forces are tangential to \mathbb{S}^3

Equilibrium



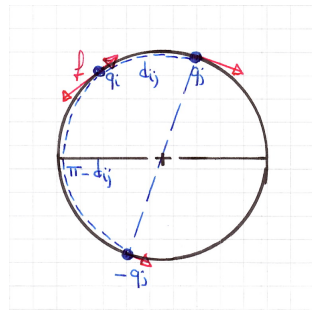
Points at 180° , $d_{ij} = 2$, $f \neq 0$



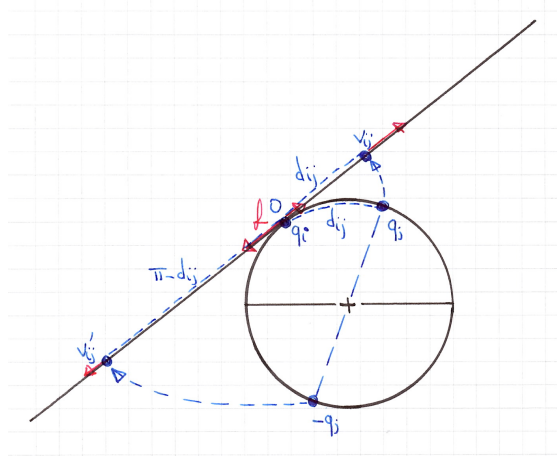
Points at 90° , $d_{ij} = \frac{\pi}{2}$ ($\Leftrightarrow \theta_{ij} = 180^\circ$), $f = 0$

Formulation in Tangent Space of Orientation Space

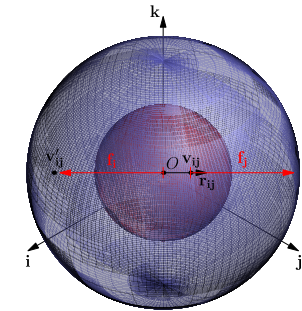
Logarithm mapping



Configuration on \mathbb{S}^3



Configuration in tangent space



Tangent space in real!

$$v_{ij} = \ln(q_j q_i^{-1}) = \frac{\theta_{ij}}{2} r_{ij} \quad v'_{ij} = -\frac{2\pi - \theta_{ij}}{2} r_{ij}$$

$$v_{ij} = d_{ij} r_{ij} \quad v'_{ij} = -(\pi - d_{ij}) r_{ij}$$

Energy and forces (discarding Coulomb's constant and the elementary charge)

$$E = 2 \left(\frac{1}{d_{ij}} + \frac{1}{\pi - d_{ij}} \right)$$

$$f_i = - \left(\frac{1}{d_{ij}^2} - \frac{1}{(\pi - d_{ij})^2} \right) r_{ij}$$

Generalization to Crystal Symmetry and N Orientations

2 orientations (reminder)

$$E = 2 \left(\frac{1}{d_{ij}} + \frac{1}{\pi - d_{ij}} \right)$$

$$f_i = - \left(\frac{1}{d_{ij}^2} - \frac{1}{(\pi - d_{ij})^2} \right) r_{ij}$$

Crystal symmetry: $\mathbf{q}^k = q \mathbf{u}^k$, $k = 1, \dots, n_c$

$$E = 2 n_c \sum_{k=1}^{n_c} \left(\frac{1}{d_{ij}^k} + \frac{1}{\pi - d_{ij}^k} \right)$$

$$f_i = - \sum_{k=1}^{n_c} \left(\frac{1}{d_{ij}^{k2}} - \frac{1}{(\pi - d_{ij}^k)^2} \right) r_{ij}^k$$

N orientations

$$E = 2 n_c \sum_{i=1}^N \sum_{j=i+1}^N \sum_{k=1}^{n_c} \left(\frac{1}{d_{ij}^k} + \frac{1}{\pi - d_{ij}^k} \right)$$

$$f_i = - \sum_{j=1, j \neq i}^N \sum_{k=1}^{n_c} \left(\frac{1}{d_{ij}^{k2}} - \frac{1}{(\pi - d_{ij}^k)^2} \right) r_{ij}^k$$

N orientations $\rightarrow O(N^2)$ CPU time to compute all f_i s

N orientations, N large ($\gtrsim 500$ for cubic symmetry)

not needed

$$f_i \simeq - \sum_{\substack{\mathbf{q} \in \left\{ \mathbf{q}_j^k, -\mathbf{q}_j^k \right\}, j \neq i \\ d(\mathbf{q}_i, \mathbf{q}) \leq \delta d_r}} \frac{1}{d(\mathbf{q}_i, \mathbf{q})^2} r(\mathbf{q}_i, \mathbf{q})$$

$\delta = 20 \equiv 8,000$ neighbours ^a $\rightarrow O(N \log N)$ CPU time
(neighbours searched by a k-d tree method)

^a depending on the termination criterion

Generalization to Crystal Symmetry and N Orientations

2 orientations (reminder)

$$E = 2 \left(\frac{1}{d_{ij}} + \frac{1}{\pi - d_{ij}} \right)$$

$$f_i = - \left(\frac{1}{d_{ij}^2} - \frac{1}{(\pi - d_{ij})^2} \right) r_{ij}$$

Crystal symmetry: $\mathbf{q}^k = q u^k$, $k = 1, \dots, n_c$

$$E = 2 n_c \sum_{k=1}^{n_c} \left(\frac{1}{d_{ij}^k} + \frac{1}{\pi - d_{ij}^k} \right)$$

$$f_i = - \sum_{k=1}^{n_c} \left(\frac{1}{d_{ij}^{k2}} - \frac{1}{(\pi - d_{ij}^k)^2} \right) r_{ij}^k$$

N orientations

$$E = 2 n_c \sum_{i=1}^N \sum_{j=i+1}^N \sum_{k=1}^{n_c} \left(\frac{1}{d_{ij}^k} + \frac{1}{\pi - d_{ij}^k} \right)$$

$$f_i = - \sum_{j=1, j \neq i}^N \sum_{k=1}^{n_c} \left(\frac{1}{d_{ij}^{k2}} - \frac{1}{(\pi - d_{ij}^k)^2} \right) r_{ij}^k$$

N orientations $\rightarrow O(N^2)$ CPU time to compute all f_i s

N orientations, N large ($\gtrsim 500$ for cubic symmetry)

not needed

$$f_i \simeq - \sum_{\substack{q \in \left\{ q_j^k, -q_j^k \right\}, j \neq i \\ d(q_i, q) \leq \delta d_r}} \frac{1}{d(q_i, q)^2} r(q_i, q)$$

$\delta = 20 \equiv 8,000$ neighbours ^a $\rightarrow O(N \log N)$ CPU time
(neighbours searched by a k-d tree method)

Generalization to Crystal Symmetry and N Orientations

2 orientations (reminder)

$$E = 2 \left(\frac{1}{d_{ij}} + \frac{1}{\pi - d_{ij}} \right)$$

$$f_i = - \left(\frac{1}{d_{ij}^2} - \frac{1}{(\pi - d_{ij})^2} \right) r_{ij}$$

Crystal symmetry: $\mathbf{q}^k = q u^k$, $k = 1, \dots, n_c$

$$E = 2 n_c \sum_{k=1}^{n_c} \left(\frac{1}{d_{ij}^k} + \frac{1}{\pi - d_{ij}^k} \right)$$

$$f_i = - \sum_{k=1}^{n_c} \left(\frac{1}{d_{ij}^{k2}} - \frac{1}{(\pi - d_{ij}^k)^2} \right) r_{ij}^k$$

N orientations

$$E = 2 n_c \sum_{i=1}^N \sum_{j=i+1}^N \sum_{k=1}^{n_c} \left(\frac{1}{d_{ij}^k} + \frac{1}{\pi - d_{ij}^k} \right)$$

$$f_i = - \sum_{j=1, j \neq i}^N \sum_{k=1}^{n_c} \left(\frac{1}{d_{ij}^{k2}} - \frac{1}{(\pi - d_{ij}^k)^2} \right) r_{ij}^k$$

N orientations $\rightarrow O(N^2)$ CPU time to compute all f_i s

N orientations, N large ($\gtrsim 500$ for cubic symmetry)

not needed

$$f_i \simeq - \sum_{\substack{q \in \left\{ q_j^k, -q_j^k \right\}, j \neq i \\ d(q_i, q) \leq \delta d_r}} \frac{1}{d(q_i, q)^2} r(q_i, q)$$

$\delta = 20 \equiv 8,000$ neighbours ^a $\rightarrow O(N \log N)$ CPU time
(neighbours searched by a k-d tree method)

^a depending on the termination criterion

Generalization to Crystal Symmetry and N Orientations

2 orientations (reminder)

$$E = 2 \left(\frac{1}{d_{ij}} + \frac{1}{\pi - d_{ij}} \right)$$

$$f_i = - \left(\frac{1}{d_{ij}^2} - \frac{1}{(\pi - d_{ij})^2} \right) r_{ij}$$

Crystal symmetry: $\mathbf{q}^k = q u^k$, $k = 1, \dots, n_c$

$$E = 2 n_c \sum_{k=1}^{n_c} \left(\frac{1}{d_{ij}^k} + \frac{1}{\pi - d_{ij}^k} \right)$$

$$f_i = - \sum_{k=1}^{n_c} \left(\frac{1}{d_{ij}^{k2}} - \frac{1}{(\pi - d_{ij}^k)^2} \right) r_{ij}^k$$

N orientations

$$E = 2 n_c \sum_{i=1}^N \sum_{j=i+1}^N \sum_{k=1}^{n_c} \left(\frac{1}{d_{ij}^k} + \frac{1}{\pi - d_{ij}^k} \right)$$

$$f_i = - \sum_{j=1, j \neq i}^N \sum_{k=1}^{n_c} \left(\frac{1}{d_{ij}^{k2}} - \frac{1}{(\pi - d_{ij}^k)^2} \right) r_{ij}^k$$

N orientations $\rightarrow O(N^2)$ CPU time to compute all f_i s

N orientations, N large ($\gtrsim 500$ for cubic symmetry)

not needed

$$f_i \simeq - \sum_{\substack{\mathbf{q} \in \left\{ \mathbf{q}_j^k, -\mathbf{q}_j^k \right\}, j \neq i \\ d(\mathbf{q}_i, \mathbf{q}) \leq \delta d_r}} \frac{1}{d(\mathbf{q}_i, \mathbf{q})^2} r(\mathbf{q}_i, \mathbf{q})$$

$\delta = 20 \equiv 8,000$ neighbours ^a $\rightarrow O(N \log N)$ CPU time
(neighbours searched by a k-d tree method)

Resolution: Gradient-descent Optimization

Evolution law (discarding the electron mass / inertial effects)

$$\text{At iteration } l: \quad \Delta q_i^{(l-1)} = \alpha^{(l-1)} f_i^{(l-1)}, \quad q_i^{(l)} = \widehat{q_i^{(l-1)} + \Delta q_i^{\star(l-1)}} \quad \text{with} \quad \Delta q_i^{\star(l-1)} = \Delta q_i^{(l-1)} q_i^{(l-1)}$$

Step size (α) for $l = 1$: value minimizing $E^{(1)}$ a priori

$$\alpha^{(0)} = 0.235 d_r^3 \quad (\text{identified once, for } N = 10^5 \text{ random orientations})$$

Step size (α) for $l > 1$: Barzilai-Borwein (BB) method (no convergence safeguard)

$$\alpha_1^{(l-1)} = \frac{\sum_{i=1}^N (\Delta q_i^{(l-2)} \cdot \Delta f_i^{(l-2)})}{\sum_{i=1}^N (\Delta f_i^{(l-2)} \cdot \Delta f_i^{(l-2)})}, \quad \alpha_2^{(l-1)} = \frac{\sum_{i=1}^N (\Delta q_i^{(l-2)} \cdot \Delta q_i^{(l-2)})}{\sum_{i=1}^N (\Delta q_i^{(l-2)} \cdot \Delta f_i^{(l-2)})}$$

Termination criterion

$$\frac{\sqrt{\sum_{i=1}^N \|f_i^{(l)}\|^2}}{\sqrt{\sum_{i=1}^N \|f_i^{(0)}\|^2}} < 10^{-3}$$

Computation time (Intel® Xeon® CPU E5-2660 v3, 20 threads)

	N	triclinic	cubic	hexagonal
10^3	3s	20s	13s	
10^4	4min	36min	22min	
10^5	17min	45min	31min	
10^6	3h30min	3h30min	3h30min	

Resolution: Gradient-descent Optimization

Evolution law (discarding the electron mass / inertial effects)

$$\text{At iteration } l: \quad \Delta q_i^{(l-1)} = \alpha^{(l-1)} f_i^{(l-1)}, \quad q_i^{(l)} = \widehat{q_i^{(l-1)} + \Delta q_i^{\star(l-1)}} \quad \text{with} \quad \Delta q_i^{\star(l-1)} = \Delta q_i^{(l-1)} q_i^{(l-1)}$$

Step size (α) for $l = 1$: value minimizing $E^{(1)}$ a priori

$$\alpha^{(0)} = 0.235 d_r^3 \quad (\text{identified once, for } N = 10^5 \text{ random orientations})$$

Step size (α) for $l > 1$: Barzilai-Borwein (BB) method (no convergence safeguard)

$$\alpha_1^{(l-1)} = \frac{\sum_{i=1}^N (\Delta q_i^{(l-2)} \cdot \Delta f_i^{(l-2)})}{\sum_{i=1}^N (\Delta f_i^{(l-2)} \cdot \Delta f_i^{(l-2)})}, \quad \alpha_2^{(l-1)} = \frac{\sum_{i=1}^N (\Delta q_i^{(l-2)} \cdot \Delta q_i^{(l-2)})}{\sum_{i=1}^N (\Delta q_i^{(l-2)} \cdot \Delta f_i^{(l-2)})}$$

Termination criterion

$$\frac{\sqrt{\sum_{i=1}^N \|f_i^{(l)}\|^2}}{\sqrt{\sum_{i=1}^N \|f_i^{(0)}\|^2}} < 10^{-3}$$

Computation time (Intel® Xeon® CPU E5-2660 v3, 20 threads)

	N	triclinic	cubic	hexagonal
10^3	3s	20s	13s	
10^4	4min	36min	22min	
10^5	17min	45min	31min	
10^6	3h30min	3h30min	3h30min	

Resolution: Gradient-descent Optimization

Evolution law (discarding the electron mass / inertial effects)

$$\text{At iteration } l: \quad \Delta q_i^{(l-1)} = \alpha^{(l-1)} f_i^{(l-1)}, \quad q_i^{(l)} = \widehat{q_i^{(l-1)} + \Delta q_i^{\star(l-1)}} \quad \text{with} \quad \Delta q_i^{\star(l-1)} = \Delta q_i^{(l-1)} q_i^{(l-1)}$$

Step size (α) for $l = 1$: value minimizing $E^{(1)}$ a priori

$$\alpha^{(0)} = 0.235 d_r^3 \quad (\text{identified once, for } N = 10^5 \text{ random orientations})$$

Step size (α) for $l > 1$: Barzilai-Borwein (BB) method (no convergence safeguard)

$$\alpha_1^{(l-1)} = \frac{\sum_{i=1}^N (\Delta q_i^{(l-2)} \cdot \Delta f_i^{(l-2)})}{\sum_{i=1}^N (\Delta f_i^{(l-2)} \cdot \Delta f_i^{(l-2)})}, \quad \alpha_2^{(l-1)} = \frac{\sum_{i=1}^N (\Delta q_i^{(l-2)} \cdot \Delta q_i^{(l-2)})}{\sum_{i=1}^N (\Delta q_i^{(l-2)} \cdot \Delta f_i^{(l-2)})}$$

Termination criterion

$$\frac{\sqrt{\sum_{i=1}^N \|f_i^{(l)}\|^2}}{\sqrt{\sum_{i=1}^N \|f_i^{(0)}\|^2}} < 10^{-3}$$

Computation time (Intel® Xeon® CPU E5-2660 v3, 20 threads)

	N	triclinic	cubic	hexagonal
10^3	3s	20s	13s	
10^4	4min	36min	22min	
10^5	17min	45min	31min	
10^6	3h30min	3h30min	3h30min	

Resolution: Gradient-descent Optimization

Evolution law (discarding the electron mass / inertial effects)

$$\text{At iteration } l: \quad \Delta q_i^{(l-1)} = \alpha^{(l-1)} f_i^{(l-1)}, \quad q_i^{(l)} = \widehat{q_i^{(l-1)} + \Delta q_i^{\star(l-1)}} \quad \text{with} \quad \Delta q_i^{\star(l-1)} = \Delta q_i^{(l-1)} q_i^{(l-1)}$$

Step size (α) for $l = 1$: value minimizing $E^{(1)}$ a priori

$$\alpha^{(0)} = 0.235 d_r^3 \quad (\text{identified once, for } N = 10^5 \text{ random orientations})$$

Step size (α) for $l > 1$: Barzilai-Borwein (BB) method (no convergence safeguard)

$$\alpha_1^{(l-1)} = \frac{\sum_{i=1}^N (\Delta q_i^{(l-2)} \cdot \Delta f_i^{(l-2)})}{\sum_{i=1}^N (\Delta f_i^{(l-2)} \cdot \Delta f_i^{(l-2)})}, \quad \alpha_2^{(l-1)} = \frac{\sum_{i=1}^N (\Delta q_i^{(l-2)} \cdot \Delta q_i^{(l-2)})}{\sum_{i=1}^N (\Delta q_i^{(l-2)} \cdot \Delta f_i^{(l-2)})}$$

Termination criterion

$$\frac{\sqrt{\sum_{i=1}^N \|f_i^{(l)}\|^2}}{\sqrt{\sum_{i=1}^N \|f_i^{(0)}\|^2}} < 10^{-3}$$

Computation time (Intel® Xeon® CPU E5-2660 v3, 20 threads)

N	triclinic	cubic	hexagonal
10^3	3s	20s	13s
10^4	4min	36min	22min
10^5	17min	45min	31min
10^6	3h30min	3h30min	3h30min

Resolution: Gradient-descent Optimization

Evolution law (discarding the electron mass / inertial effects)

$$\text{At iteration } l: \quad \Delta q_i^{(l-1)} = \alpha^{(l-1)} f_i^{(l-1)}, \quad q_i^{(l)} = \widehat{q_i^{(l-1)} + \Delta q_i^{\star(l-1)}} \quad \text{with} \quad \Delta q_i^{\star(l-1)} = \Delta q_i^{(l-1)} q_i^{(l-1)}$$

Step size (α) for $l = 1$: value minimizing $E^{(1)}$ a priori

$$\alpha^{(0)} = 0.235 d_r^3 \quad (\text{identified once, for } N = 10^5 \text{ random orientations})$$

Step size (α) for $l > 1$: Barzilai-Borwein (BB) method (no convergence safeguard)

$$\alpha_1^{(l-1)} = \frac{\sum_{i=1}^N (\Delta q_i^{(l-2)} \cdot \Delta f_i^{(l-2)})}{\sum_{i=1}^N (\Delta f_i^{(l-2)} \cdot \Delta f_i^{(l-2)})}, \quad \alpha_2^{(l-1)} = \frac{\sum_{i=1}^N (\Delta q_i^{(l-2)} \cdot \Delta q_i^{(l-2)})}{\sum_{i=1}^N (\Delta q_i^{(l-2)} \cdot \Delta f_i^{(l-2)})}$$

Termination criterion

$$\frac{\sqrt{\sum_{i=1}^N \|f_i^{(l)}\|^2}}{\sqrt{\sum_{i=1}^N \|f_i^{(0)}\|^2}} < 10^{-3}$$

Computation time (Intel® Xeon® CPU E5-2660 v3, 20 threads)

N	triclinic	cubic	hexagonal
10^3	3s	20s	13s
10^4	4min	36min	22min
10^5	17min	45min	31min
10^6	3h30min	3h30min	3h30min

Orientation Evolution (1000 orientations)

No symmetry

Orientations

ODF (f)

$$\sigma_f = \sqrt{\frac{1}{2\pi^2} \int_{\mathbb{S}^2} (f(q) - 1)^2 ds}$$

Orientation Evolution (1000 orientations)

Cubic symmetry

Cubic symmetry with 82 fixed orientations ($\langle 100 \rangle$ and $\langle 110 \rangle$ fibres)

Orientations

ODF (f)

Hexagonal symmetry

Orientations

ODF (f)

Orientations

ODF (f)

Outline

Generation of Microstructures

Meshing

Simulation and Post-processing

Visualization

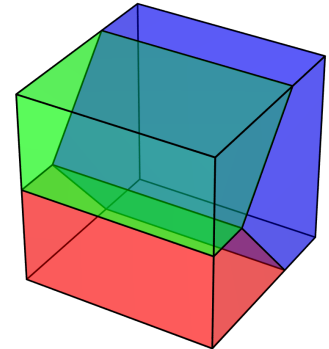
Conclusions

A Bottom-Up Flow

Principle

- 0D meshing: all vertices
- 1D meshing: all edges
- 2D meshing: all faces (constrained by the 1D mesh)
- 3D meshing: all polyhedra (constrained by the 2D mesh)

2D/3D meshing: Gmsh and Netgen

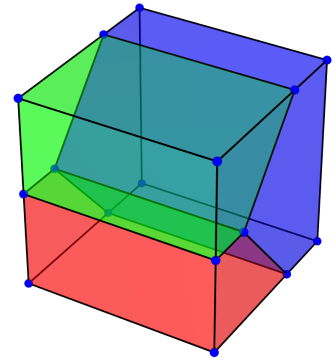


A Bottom-Up Flow

Principle

- 0D meshing: all vertices
- 1D meshing: all edges
- 2D meshing: all faces (constrained by the 1D mesh)
- 3D meshing: all polyhedra (constrained by the 2D mesh)

2D/3D meshing: Gmsh and Netgen

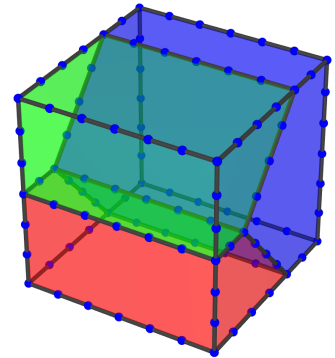


A Bottom-Up Flow

Principle

- 0D meshing: all vertices
- 1D meshing: all edges
- 2D meshing: all faces (constrained by the 1D mesh)
- 3D meshing: all polyhedra (constrained by the 2D mesh)

2D/3D meshing: Gmsh and Netgen

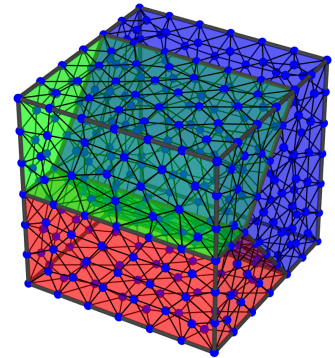


A Bottom-Up Flow

Principle

- 0D meshing: all vertices
- 1D meshing: all edges
- 2D meshing: all faces (constrained by the 1D mesh)
- 3D meshing: all polyhedra (constrained by the 2D mesh)

2D/3D meshing: Gmsh and Netgen

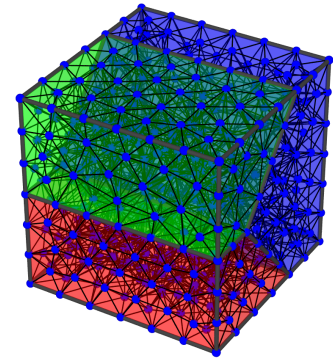


A Bottom-Up Flow

Principle

- 0D meshing: all vertices
- 1D meshing: all edges
- 2D meshing: all faces (constrained by the 1D mesh)
- 3D meshing: all polyhedra (constrained by the 2D mesh)

2D/3D meshing: Gmsh and Netgen

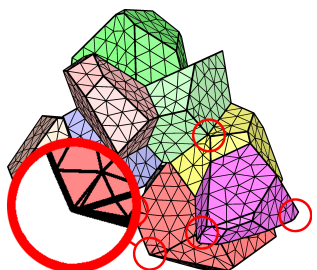
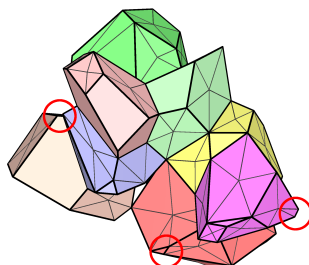
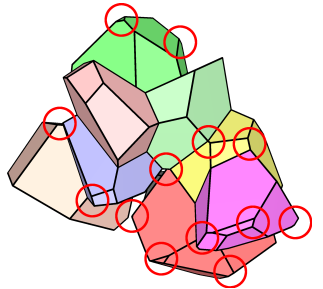


Problems with large polycrystals / large strains

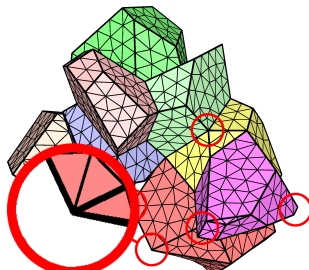
- Geometrical details → regularization
- Randomness → multimeshing
- Strong deformation heterogeneity → remeshing

Regularization

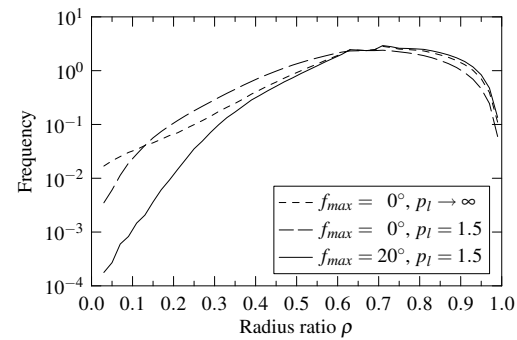
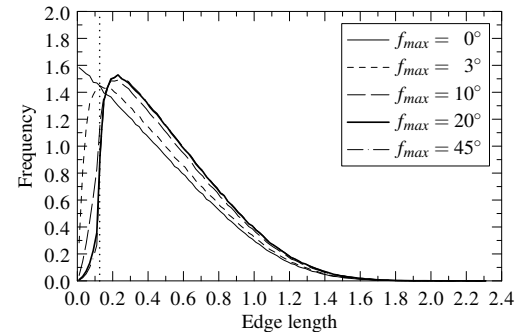
Principle and results



bad-quality (sliver) elements



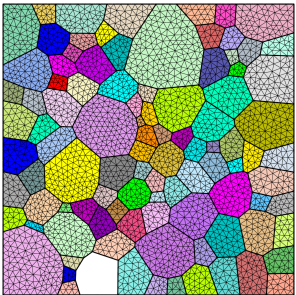
good-quality elements



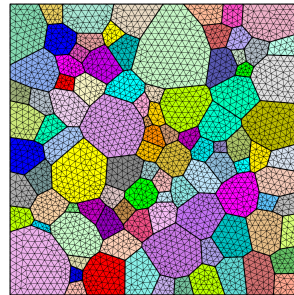
Multimeshing

Motivation: many grains + infinite variety of grain shapes + several meshing algorithms available

Principle: concurrent use of several meshing algorithms



Mesher 1 (Delaunay)



Mesher 2 (Frontal)

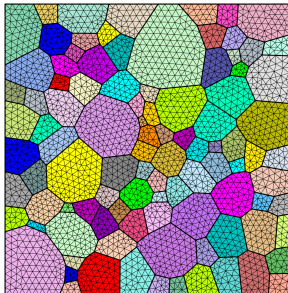
- Grains are meshed independently using several methods
- For each grain, the best-quality mesh is used

$$O = O_{dis}^{1-\alpha} O_{size}^{\alpha} \quad (O \in [0, 1]) \quad \text{with } \alpha = 0.2$$

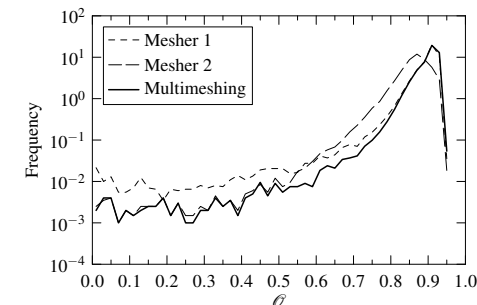
$$O_{dis} = \prod_{i=1}^{n_e} \sigma_i \quad \text{where} \quad \begin{cases} \text{if } \rho_i < 1, \sigma_i = \rho_i^{\exp\left(\frac{\rho_i^{0.01}}{\rho_i^{0.01}-1}\right)} \\ \text{if } \rho_i = 1, \sigma_i = 1 \end{cases} \quad (\rho_i: \text{radius ratio})$$

$$O_{size} = \left(\frac{1}{n_e} \sum_{i=1}^{n_e} \nu_i \right)^3 \quad \text{where} \quad \begin{cases} \text{if } l_i < c_l, \nu_i = l_i/c_l \\ \text{if } l_i \geq c_l, \nu_i = c_l/l_i \end{cases}$$

Results



Multimeshing (60% mesher 1, 40% mesher 2)



Robustness + very few poor-quality elements ($\rho < 0.05 \rightarrow 5-10 / 10^6$ elements)

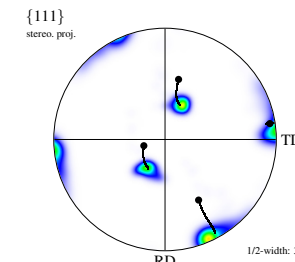
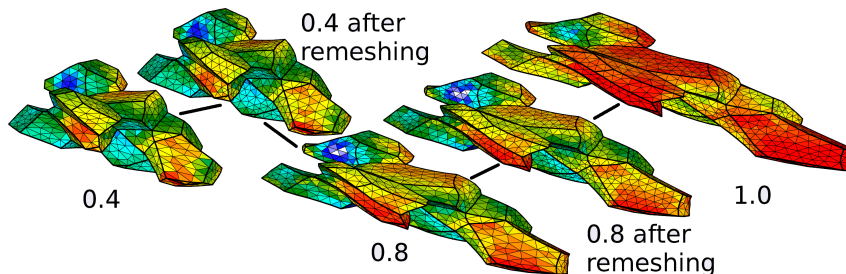
Remeshing

Principle: very similar to meshing, but with **curved** edges and faces

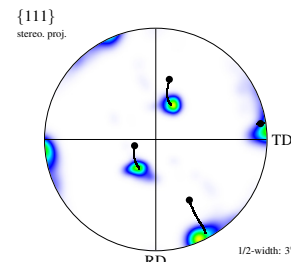
- 0D remeshing = 0D meshing
- 1D remeshing = 1D meshing, but in curvilinear coordinates
- 2D remeshing: old mesh projection in a mean plane, 2D meshing, new mesh backprojection
- 3D remeshing = 3D meshing
- Transport of state variables (zero'ing stresses)

Remaining difficulties: very deformed faces (keeping the old mesh) and overlapping faces (no trivial solution — limiting ε to ~ 1.5)

Results

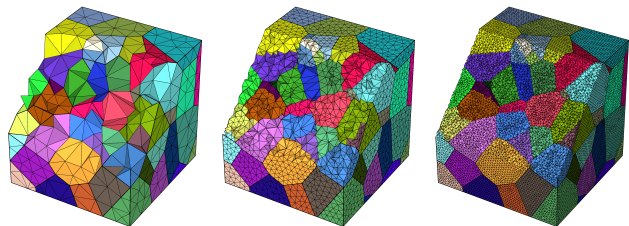


Infrequent remeshing

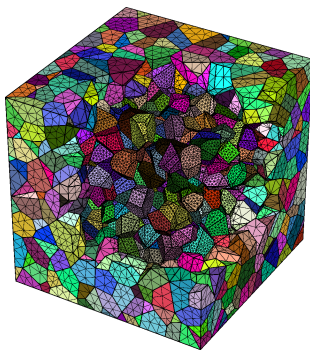


Frequent remeshing

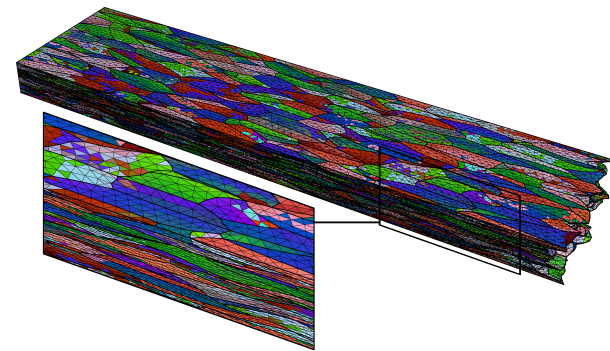
Examples



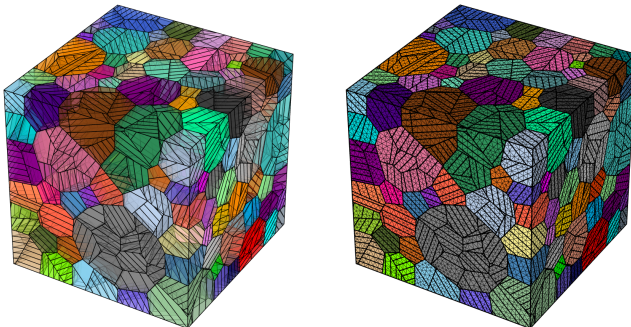
Different element sizes



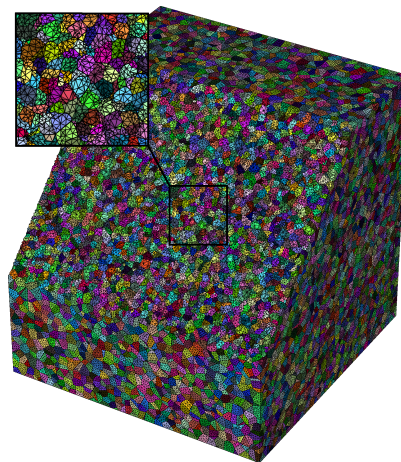
2000-grain polycrystal with finely meshed central grains



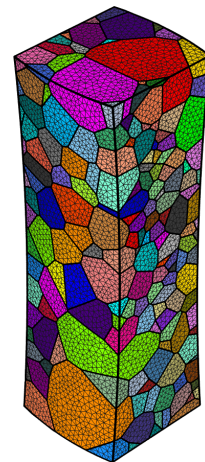
3000-grain polycrystal, $\varepsilon = 1.4$



Bainite polycrystal and its mesh



100,000 grains, 19,600,000 elements, 26,400,000 nodes



Real polycrystal, non-convex

Outline

Generation of Microstructures

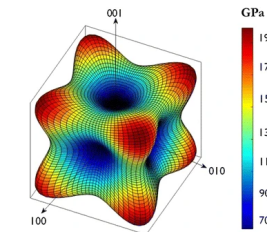
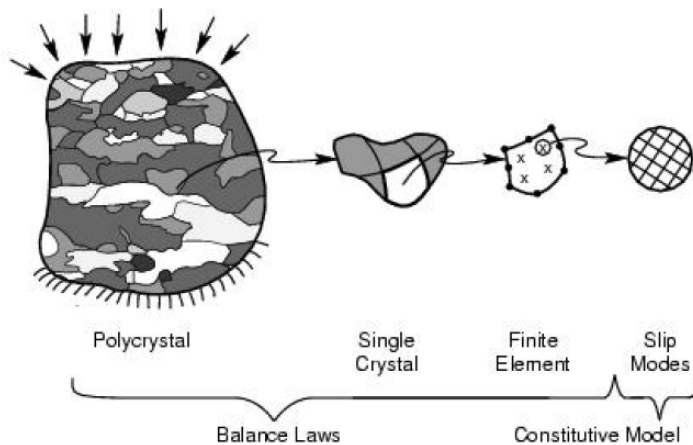
Meshing

Simulation and Post-processing

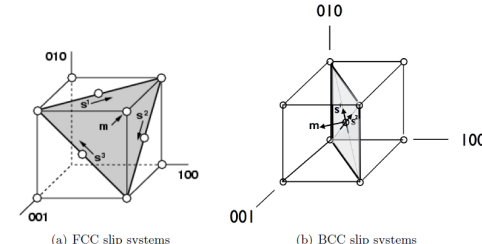
Visualization

Conclusions

Principle

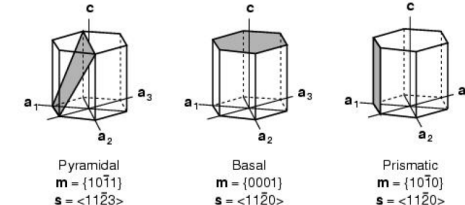


Crystal elasticity



(a) FCC slip systems

(b) BCC slip systems



Anisotropic plasticity

Specificities

- Small and large strains
- Large-scale polycrystals (parallelization)
- Mechanical loading only (no heat transfer or other physical processes)
- No fracture
- Simple boundary conditions (no friction or changing contact conditions)

Crystal structure

- FCC, BCC

- HCP

- Other (for rocks)

(multiphase allowed)

Anisotropic elasticity

Cubic crystal symmetry

$$\begin{pmatrix} \sigma_{11} \\ \sigma_{22} \\ \sigma_{33} \\ \sigma_{23} \\ \sigma_{13} \\ \sigma_{12} \end{pmatrix} = \begin{bmatrix} C_{11} & C_{12} & C_{12} \\ C_{12} & C_{11} & C_{12} \\ C_{12} & C_{12} & C_{11} \\ C_{12} & C_{12} & C_{11} \\ C_{44} & & C_{44} \\ & C_{44} & C_{44} \end{bmatrix} \begin{pmatrix} \epsilon_{11} \\ \epsilon_{22} \\ \epsilon_{33} \\ 2\epsilon_{23} \\ 2\epsilon_{13} \\ 2\epsilon_{12} \end{pmatrix}$$

Hexagonal crystal symmetry

$$\begin{pmatrix} \sigma_{11} \\ \sigma_{22} \\ \sigma_{33} \\ \sigma_{23} \\ \sigma_{13} \\ \sigma_{12} \end{pmatrix} = \begin{bmatrix} C_{11} & C_{12} & C_{13} \\ C_{12} & C_{11} & C_{13} \\ C_{13} & C_{13} & C_{11} \\ C_{44} & & C_{44} \\ & C_{44} & C_{44} \\ & & (C_{11} - C_{12})/2 \end{bmatrix} \begin{pmatrix} \epsilon_{11} \\ \epsilon_{22} \\ \epsilon_{33} \\ 2\epsilon_{23} \\ 2\epsilon_{13} \\ 2\epsilon_{12} \end{pmatrix}$$

Crystal plasticity

$$\dot{\gamma}^\alpha = \dot{\gamma}_0 \left(\frac{|\tau^\alpha|}{g^\alpha} \right)^{\frac{1}{m}} \operatorname{sgn}(\tau^\alpha)$$

Isotropic hardening

$$\dot{g}^\alpha = h_0 \left(\frac{g_{s0} - g^\alpha}{g_{s0} - g_0} \right)^n \dot{\gamma} \quad \text{where} \quad \dot{\gamma} = \sum_\alpha |\dot{\gamma}^\alpha|$$

$$\dot{g}^\alpha = h_0 \left(\frac{g_s(\dot{\gamma}) - g^\alpha}{g_s(\dot{\gamma}) - g_0} \right)^n \dot{\gamma}, \quad g_s(\dot{\gamma}) = g_{s0} \left(\frac{\dot{\gamma}}{\dot{\gamma}_{s0}} \right)^{m'}$$

Isotropic, cyclic hardening

$$\dot{g}^\alpha = h_0 \left(\frac{g_s(\dot{\gamma}) - g^\alpha}{g_s(\dot{\gamma}) - g_0} \right)^n f,$$

$$f = \sum_{\beta=0}^{n_a} |\dot{\gamma}^\beta|$$

$$\Delta\gamma_{crit} = a [g/g_s(\dot{\gamma})]^c,$$

Anisotropic hardening

$$\dot{g}^\alpha = h_0 \left(\frac{g_s(\dot{\gamma}) - g^\alpha}{g_s(\dot{\gamma}) - g_0} \right)^n \dot{\gamma} h_{\alpha\beta},$$

Various loadings

- Uniaxial loading / strain or force controlled
- Multiaxial loading
- Custom loading
- Cyclic loading
- Strain rate jumps, load rate jumps, dwell episodes...

Restart

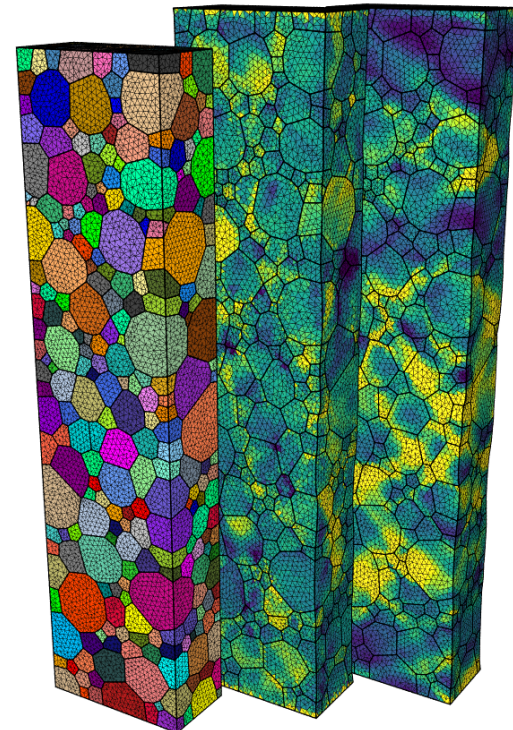
- For cyclic simulations (add cycles)
- For large strain simulations (after remeshing)
- For incomplete simulations (add deformation)
- In the case of premature failure (wall time limit, power outage, etc.)

Nodes

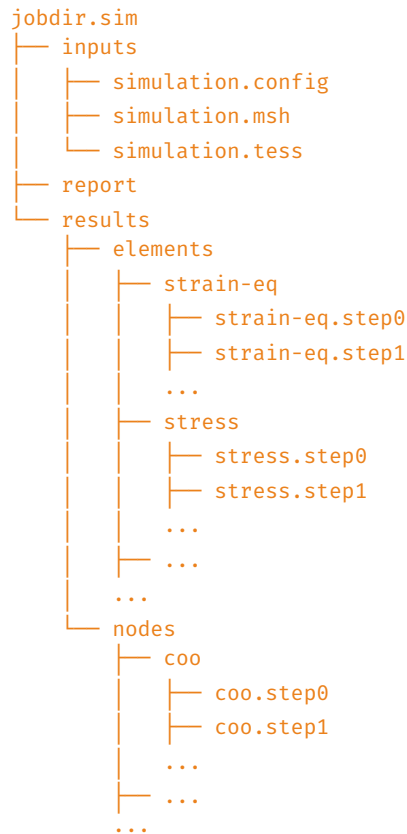
- Position
- Displacement
- Velocity

Elements

- Resolved shear stresses
- Slip rates, slips
- Elastic strain tensor, plastic strain tensor, total strain tensor
- Stress tensor
- Deformation rate (total and plastic) tensor, spin rate tensor, velocity gradient
- Work rate, work (total and plastic)
- Fiber-averaged results



Simulation directory



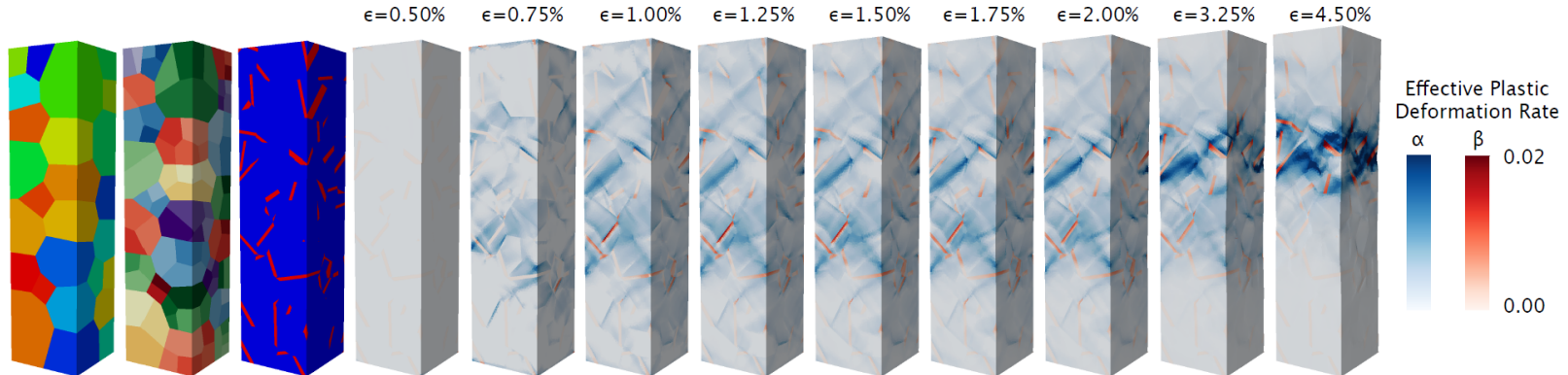
Post-processing

- New variables, mesh or simulation based
("vol, stress33, myvar:crss-crss(step=0)")
 - Grain averaging and other statistical treatments
 - Efficient result management (deletion, update, etc.)

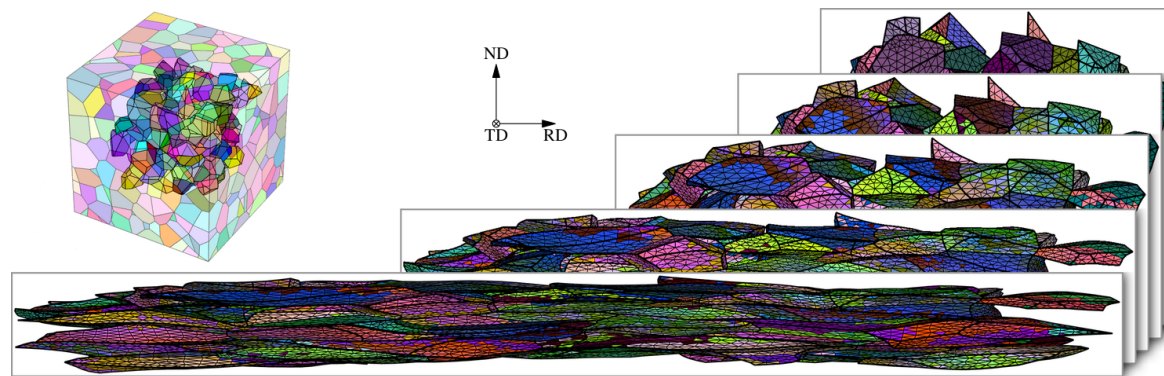
To come

- More built-in variables
 - Support of experimental data (HEXD)
 - Definition of ROIs
 - Extraction of results at specific points (e.g. on a grid)
 - ...

Simulation Examples



Deformation of Ti64 (Kasemer et al, 2017)



Large deformation of Al (Quey et al, 2011)

Outline

Generation of Microstructures

Meshing

Simulation and Post-processing

Visualization

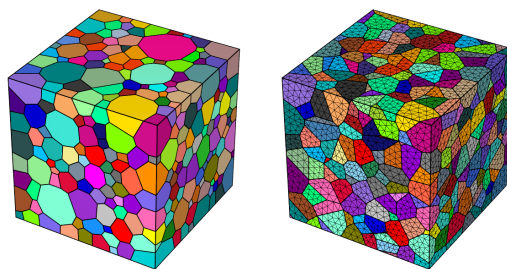
Conclusions

Visualization

Top-quality / publication-quality rendering in PNG (or VTK)

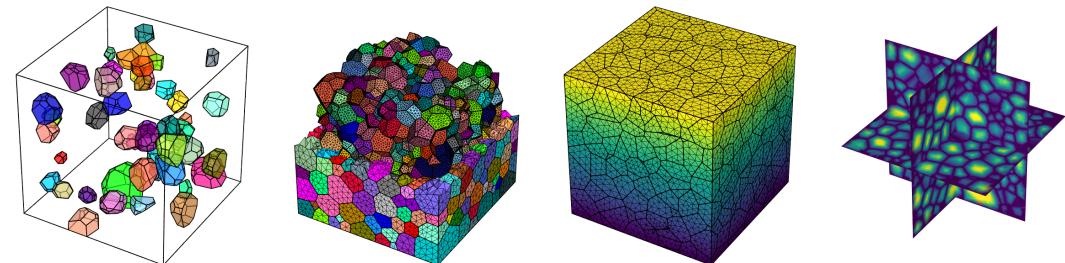
Ray-tracing with full control of the scene: camera position and angle, projection, light, additional objects, image size, etc.

Tessellation and mesh



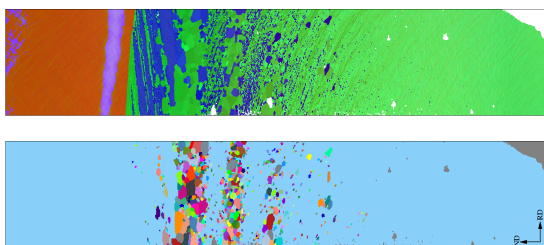
Tessellation, mesh

Entity selection, transparency, slicing...



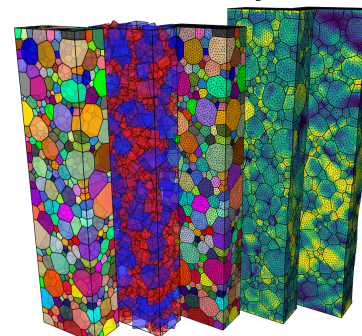
Selected cells, selected elsets, colored elements, sliced mesh

EBSD map



Orientation field and cell field (matrix / nuclei)

Simulation directory



Tessellation, phase, mesh, equivalent stress, equivalent strain

Outline

Generation of Microstructures

Meshing

Simulation and Post-processing

Visualization

Conclusions

Conclusions

Neper/FEPX

- A lively collaborative project!
- Methods described in dedicated papers:
 - (Quey, Dawson and Barbe, CMAME, 2011)
 - (Quey and Renversade, CMAME, 2015)
 - (Quey, Villani and Maurice, JAC, 2018)
 - (Dawson and Boyce, arXiv, 2015)
- Websites: <https://neper.info>, <https://fepx.info>
- Extensive documentations (130 and 70 pages)
- GitHub repositories for user interaction (Discussions, Issues)
- 350 application papers on metals, rocks, ice, 2D materials, in mechanics, magnetism, diffusion, wave propagation, etc.

Contributions are welcome!

deformation movie

Workflow

